

6. RESULT AND DISCUSSION:**6.1 Preformulation study data of Bendamustine loaded Chitosan and PLGA nanoparticle:****6.1.1 Physical and morphological Evaluation**

The pure drug bendamustine was appeared as off-white colored microcrystalline powder with amphoteric properties. The melting point was found to be 150⁰C. The official range stated in literature is 150-154⁰C. Results are given in table.no 1.8.

Table.1.9: Physical and morphological properties of Bendamustine:

Sr.no	Property	Observation
1	State	Microcrystalline powder
2	Color	Off- white
3	Odor	Odorless
4	Melting Point	152 ⁰ C

6.1.2 Solubility study

The bendamustine is freely soluble in methanol and partially soluble in water. The result of solubility is depicted in table1.10

Table.1.10: solubility study of bendamustine

Solvent	Solubility	Inference
Distilled water	1 part of solute is soluble in 30 parts of solvent.	Sparingly soluble
Chloroform	1 part of solute in more than 10000 parts of solvent.	Insoluble
Dichloromethane	1 part of solute in 20 parts of solvent.	Soluble
Acetone	1 part of solute in more than 10000 parts of solvent.	Insoluble
Ethanol	1 part of solute in 20 parts of solvent.	Soluble
Methanol	1 part of solute in 10 parts of solvent.	Freely soluble
Iso- propanol	1 part of solute in 20 parts of solvent	Soluble

6.1.3UV-Visible Spectroscopy study

6.1.3.1 Absorption maxima and standard curve

A UV absorption maximum of BM in methanol was calculated by scanning the solution (40µg/ml) of BM from 200 nm to 430 nm by UV-Spectrophotometer. The maximum absorbance of BM solution was recorded 329 nm in methanol. The standard calibration curve of BM was prepared in solvent methanol in the concentration of 4-40 µg/ml with good correctness for methanol. The absorption maximum of BM in methanol is shown in figure.1.10

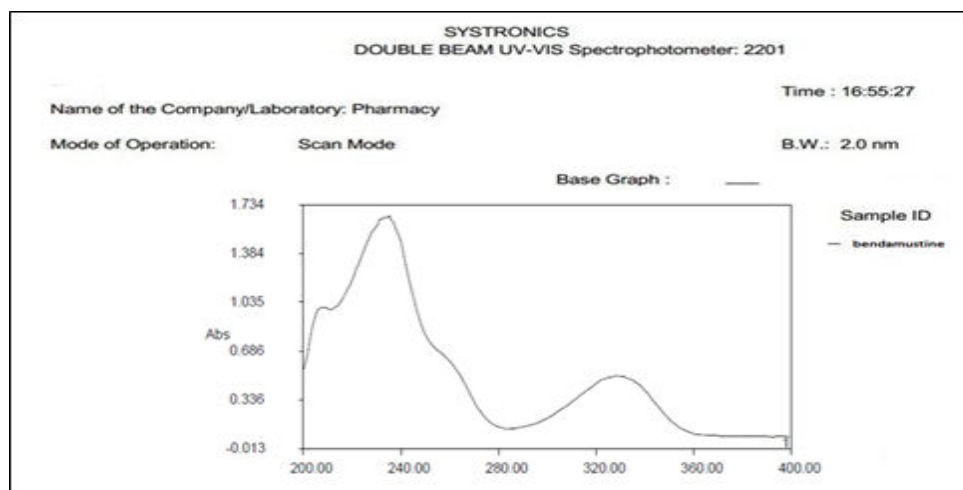


Figure.1.10: Standard calibration curve of bendamustine

6.1.3.2 Calibration curve of BM

The calibration curve of bendamustine was accessed in methanol by using UV-spectrophotometer. The prepared drug solutions of concentration ranging 4-40 $\mu\text{g/ml}$ were scanned at λ_{max} (absorbance maxima) 329 nm and the absorbance was determined. The data are shown in Table 1.10. The calibration curve of BM is shown in figure.1.11

Table.1.11: Absorbance of bendamustine solution at 329nm:

S. No.	Concentration (µg/ml)	Absorbance
1.	4	0.136
2.	8	0.236
3.	12	0.332
4.	16	0.426
5.	20	0.534
6.	24	0.639
7.	28	0.728
8.	32	0.832
9.	36	0.924
10.	40	1.028

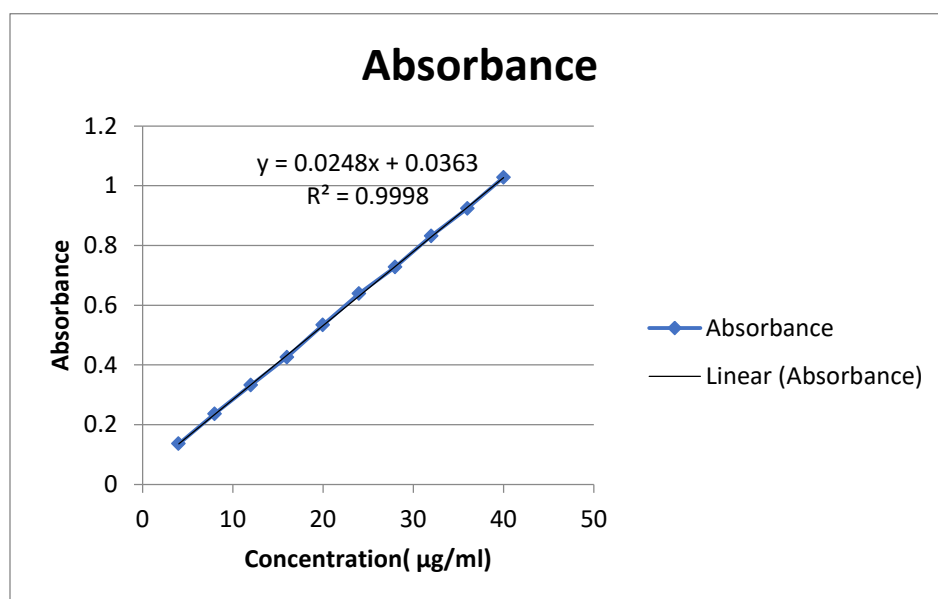


Figure 1.11: Calibration curve of Bendamustine

6.1.4 FTIR Spectra of pure drug and Excipients (for chitosan bendamustine nanoparticle):

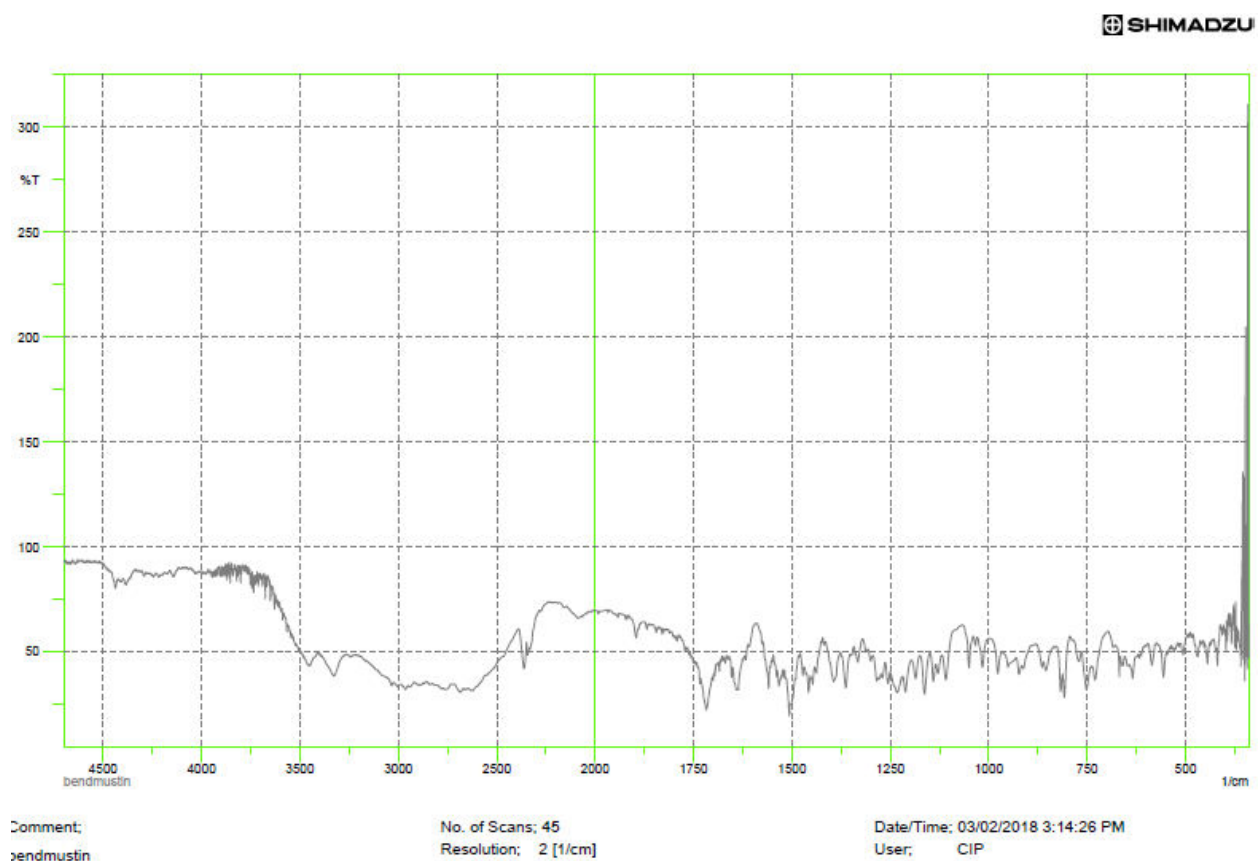


Figure 1.12: FTIR Spectra of Bendamustine

The FTIR spectra of BM explained which show distinguishing peaks at 3315 cm^{-1} due to O-H stretching bond, at 2715.01 cm^{-1} C-H stretching, 1502.60 cm^{-1} , N-CH₃ stretching and 1634.06 cm^{-1} C=C stretching. The peaks are as shown in Figure 1.12 and Table 1.11, which gives the distinguishing absorption of different functional groups of drugs.

Table. 1.12: Important absorptionpeaks of bendamustine

Functional group	Observed wave number (cm ⁻¹)
-OH stretching	3315
-C-H stretching	2715 .01
C=C stretching	1650.06
-N-CH3 stretching	1502.60

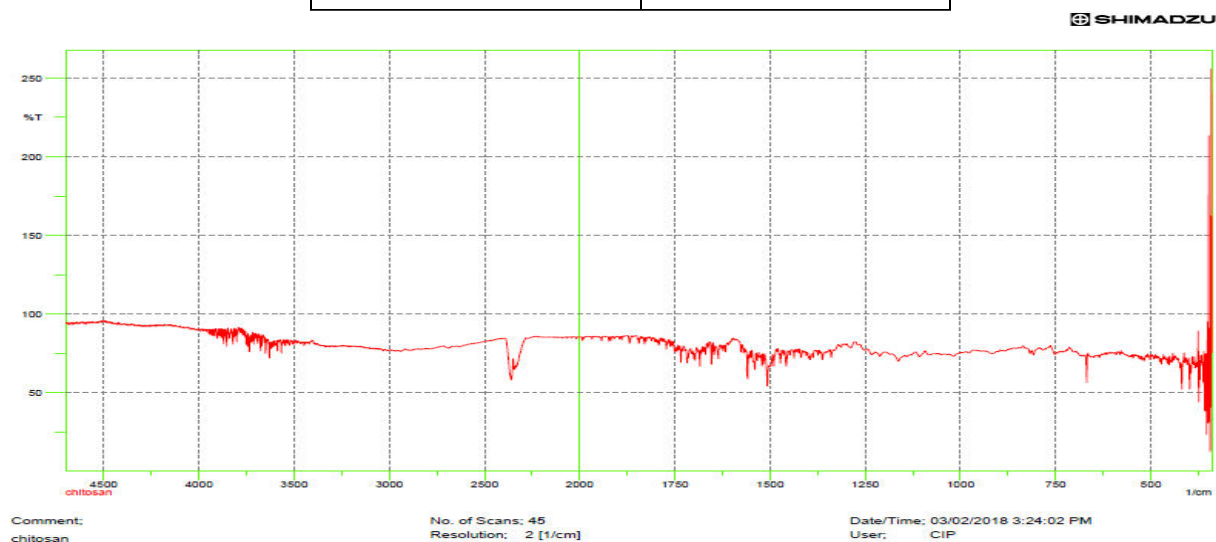


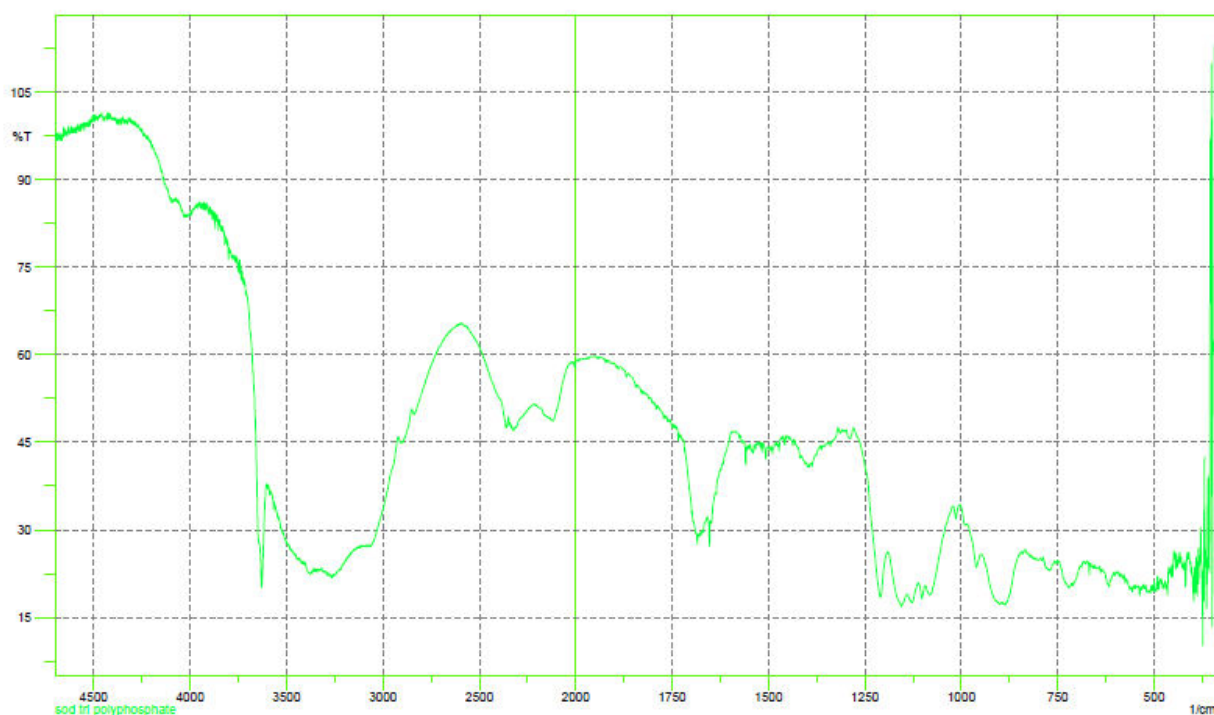
Figure 1.13: FTIR Spectra of Chitosan

An FTIR spectrum of chitosan was characterized by typical absorption band at about 3478.68cm⁻¹ (-OH stretching). The absorption peaks at about 1656.80cm⁻¹, 1571 and 1422.53cm⁻¹ were related to occurrence of C=O stretching of the amide I band with bending vibrations of N-H amide II band, C-H bending, OH bending respectively.

Table.1.13: Important peaks of Chitosan

Functional group	Observed wave number (cm ⁻¹)
-OH stretching	3478.68
C=O stretching	1656.80
N-H bending	1571
C-H bending	1422
OH bending	1376.18

SHIMADZU



Comment:
sod tri polyphosphate

No. of Scans; 45
Resolution; 2 [1/cm]

Date/Time; 03/02/2018 2:47:30 PM
User; CIP

Figure 1.14: FTIR Spectra of TPP

In the FTIR spectra of TPP distinguishing bands were observed at 1211 cm^{-1} (P = O stretching), 1145 cm^{-1} symmetric and asymmetric stretching vibrations in PO_2 group, 1087 cm^{-1} and 865 cm^{-1} stretching of P-O-P bridge.

6.1.5 Drug Excipient compatibility study by FTIR:

In order to find out the interaction/compatibility between BM, selected polymer (Chitosan), selected surfactant (TPP), FTIR spectra were recorded and the major peaks were determined. The spectra of mixtures of BM with chitosan, TPP showed the occurrence of typical peaks of the drug (BM) at 3414.8 cm^{-1} O-H group stretching, 2953.01 cm^{-1} C-H group stretching, 1502.60 cm^{-1} N- CH_3 stretching and 1634.06 cm^{-1} C=C stretching of aromatic with slight variation or shifting in the peaks.

The spectrum of bendamustine with the selected excipients (Chitosan, TPP) respectively showed all the characteristic peaks of BM with no additional or new peaks other than peaks of individual components. This indicates the compatibility of BM with selected excipients.

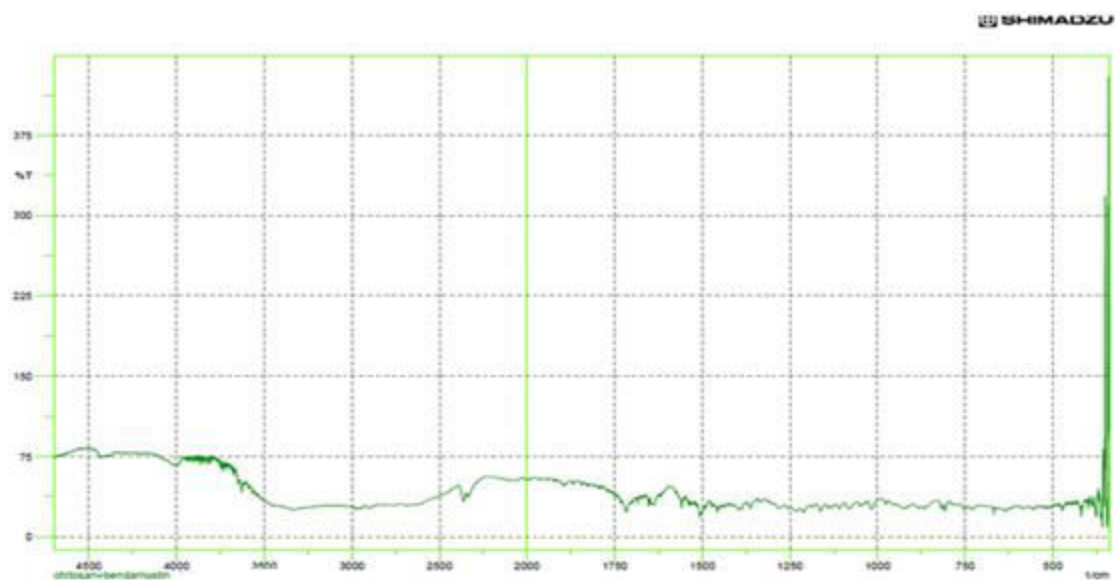


Figure 1.16: FTIR Spectra of Bendamustine with Chitosan

FTIR Spectra of drug and Excipients (for bendamustine loaded PLGA nanoparticle):

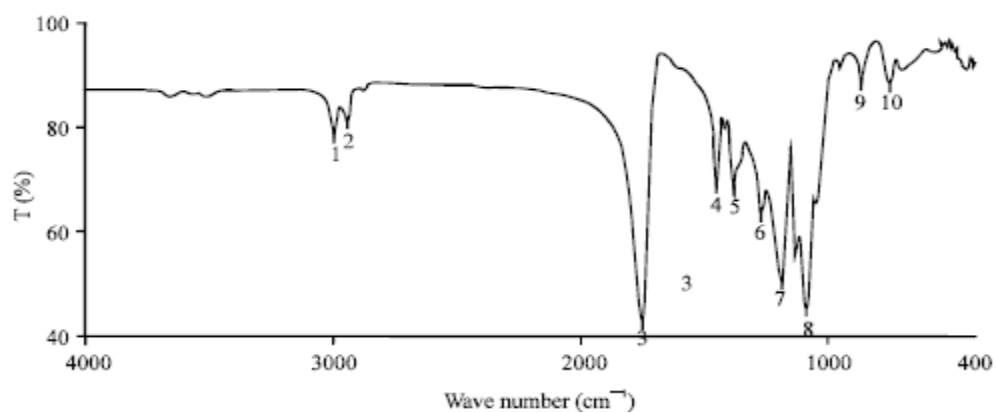


Figure 1.17: FTIR Spectra of PLGA

The FTIR spectra of PLGA showed the typical absorption peaks of -CH , -CH_2 , -CH_3 stretching at approximate range of $2850\text{-}3050\text{ cm}^{-1}$, C-O stretching at $1020\text{-}1270\text{ cm}^{-1}$, and carbonyl group C=O stretching in the range between $1700\text{-}1800\text{ cm}^{-1}$. The figure 1.17 shows the FTIR spectra of PLGA.

Table.1.14: Important peaks of PLGA

Functional group	wave number(cm^{-1})
OH- stretch	3512
-CH- stretch	2995
C=O stretch	1757
C-O stretch	1368
C-C stretch	868

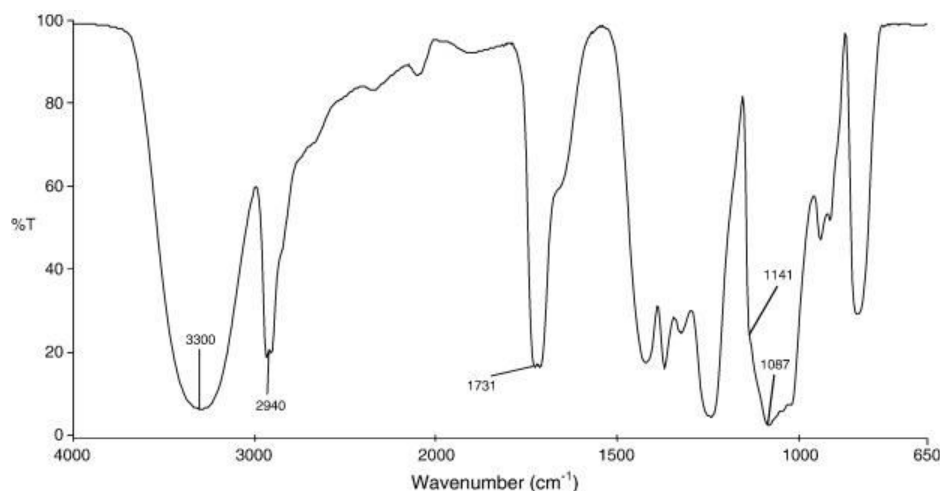
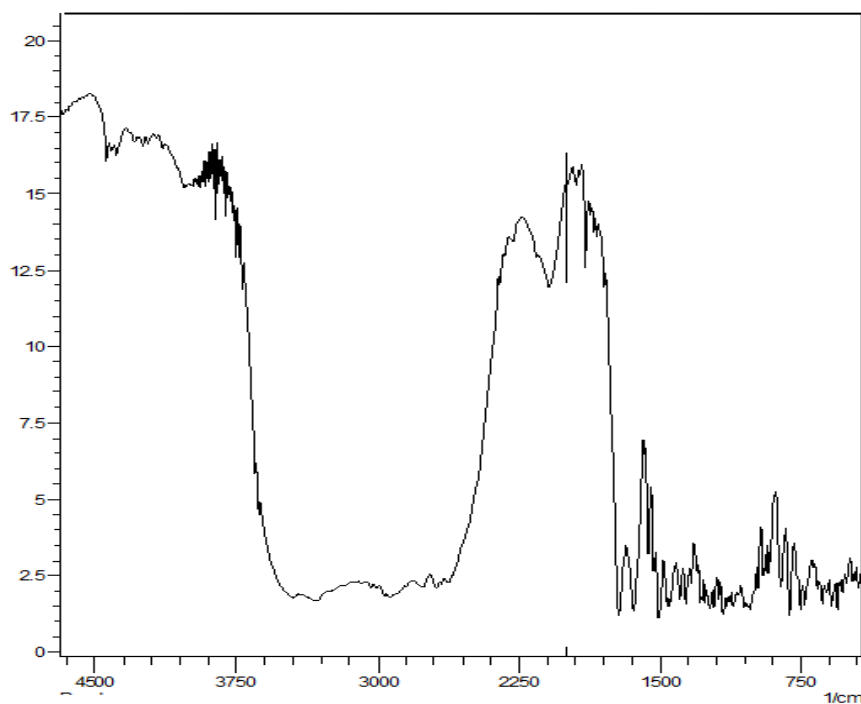


Figure 1.18: FTIR Spectra of PVA

The FTIR spectra of PVA showed peaks related to hydroxyl and acetate groups. The many bands observed inside 3550 and 3200 cm^{-1} are correlated to stretching of O-H group and the intra-molecular and intermolecular hydrogen bonds. Findings suggest between $2840\text{-}3000\text{ cm}^{-1}$ the

stretching of C-H group (alkyl group) and at $1750-1735\text{ cm}^{-1}$ is due to the stretching of C=O, C-O (acetate group).

In order to study the compatibility between BM, selected polymer PLGA and other excipients like PVA, acetone, dichloromethane the spectra was recorded and the main peaks were determined. The spectra of mixtures of BM with PLGA, PVA, acetone and dichloromethane showed the occurrence of typical peaks of the drug peaks (BM) at 3414.8 cm^{-1} due to O-H group stretching, at 2953.01 cm^{-1} C-H group stretching of aliphatic, 1502.60 cm^{-1} N-CH₃ functional group stretching and 1634.06 cm^{-1} C=C stretching of aromatic with slight shifting or variation in the peaks. Though, no additional or new peaks were observed that clarifies the pure drug was completely compatible with all the selected excipients. The IR spectra of BM with PLGA, PVA are depicted in figure no. 1.19 to 1.20.



Some important characteristic absorption peak of compatibility between BM and PLGA

Table.1.15: Important peaks obtained from BM and PLGA interaction

Functional group	wave number (cm ⁻¹)
OH- stretching	3415.8
C-H stretching	2952.01
C=C stretching	1631.06
N-CH ₃ stretching	1502.6
CH ₂ stretching	2840
CH ₃ stretching	3050
C-O stretching	1135
C=O stretching	1765

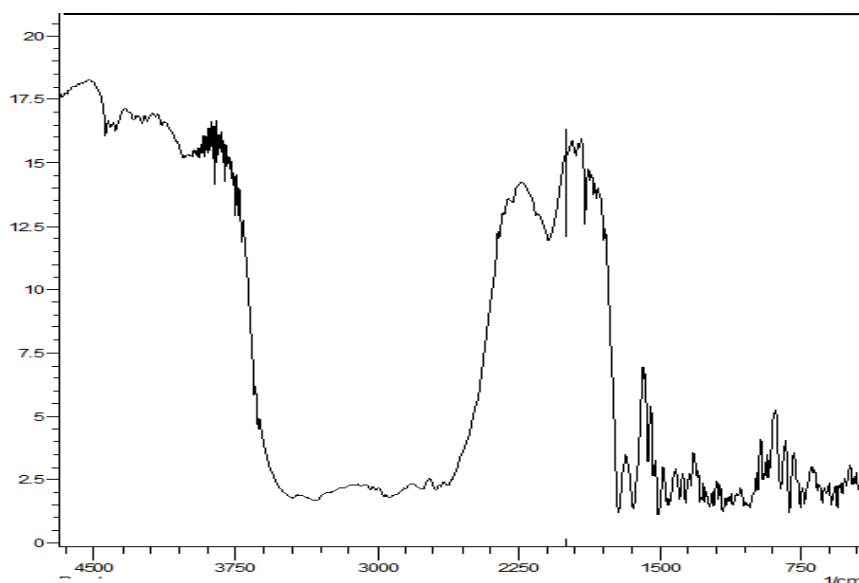


Table.1.16: Some characteristic peaks obtained from BM and PVA interaction:

Functional group	Wave number (cm ⁻¹)
OH- stretching	3415.8
C-H stretching	2952.01
C=C stretching	1631.06
N-CH ₃ stretching	1502.6
CH ₂ stretching	2840
C-O stretching	1135
C=O stretching	1764

6.1.6 Partition Coefficient:

The partition coefficient of bendamustine was estimated 4.2. The observed results are depicted in table 1.16 Results of partition coefficient value of BM confirmed its lipophilic nature.

Table.1.17: Partition coefficient of Bendamustine

S. No.	Medium	Partition coefficient(n-octanol/aq. Phase)
1.	n-Octanol: Water	4.2
2.	n-Octanol: PBS pH (7.4)	3.8

6.2 Preparation of Chitosan Nanoparticles:

Chitosan nanoparticle was successfully prepared through ionic gelation method. The master formula for the preparation depicted in the table. 1.17.

Table.1.18: The formula for the preparation of chitosan nanoparticles

Sr. No	Name of Ingredient	Quantity
1.	Chitosan	5mg/ml
2.	Sodium Tripolyphosphate	1%w/v
3	Methanol	5ml
4.	Mannitol	1%
5.	Water	10ml
Conditions		
Sonication time	5-7 min	
Sonication time	5 minutes	
Temperature	Room temperature	

6.3 Optimization of Chitosan nanoparticle:

In the Optimization process firstly, Preliminary studies were done to determine the suitable range of polymer and surfactant for the formation of nanoparticles with the drug. Different concentrations of polymer i.e. 0.1-0.75% w/v of chitosan and surfactant 0.5-1.0% w/v were taken for the preparation of chitosan nanoparticles through ionic gelation method. The results revealed that within selected range of polymer and surfactant concentration demonstrated three kinds of phenomena i.e. solution, with low and high concentration of polymer and surfactant were further observed for formation of optimum nanocarriers through design expert software. So, the result of key variables of particle size and other physiochemical parameters of nano sized particles were studied primarily for finding the correct ratio that result in nanoparticle of small

size of nano range by means of constricted size distribution. Table 1.18 shows selected formulations of chitosan nanoparticles particle size and their entrapment efficiency.

Table.1.19: Formulations of Chitosan Nanoparticles Particle Size And Their Entrapment Efficiency

Nanoparticle formulation no.	Particle size (nm)	Entrapment efficiency %
NPS1	140.12±4.2	60.18±0.16
NPS2	110.51±6.2	50.01±0.21
NPS3	124.12±2.3	53.05±0.19
NPS4	130.27±3.4	64.11±0.13
NPS5	145.09±3.5	61.15±0.17
NPS6	151.15±4.1	63.16±0.23
NPS7	137.19±3.6	57.12±0.20
NPS8	160.09±5.1	63.18±0.12

6.3.1 Effects on Particle Size of Chitosan Nanoparticle

The particle size of 8 batches of Chitosan nanoparticle ranged from 110.51±6.2 nm to 169±5.1 nm for three factors, two level combinations. The following quadratic equation described the influence of independent variables on particle size:

$$Y_1 \text{ (Particle size)} = 130.70 + 9.22A + 7.34B - 6.12C + 1.67AB - 0.65AC - 0.48BC + 22.43A^2 + 27.11B^2 + 17.18C^2$$

From this equation that was clear through increased concentration of polymer particle size quickly increased where as it also implicates that increased polymer concentration gave positive effect on particle size. The considerable enhancement of polymer concentration may be attributed to the increase in the quantity of chitosan chains for the dispensation of bigger particles once stimulated by TPP a cross linking agent. It is also notable that decreased cross linking density between chitosan and TPP, resulted particle accumulation and formation of large particles. Similarly, it also implicated that elevated concentration level of TPP encourages a quicker cross linking observable fact that may be the reason for particle size improvement. The negative value before coefficient C shows increased sonication time would decrease the particle size. Increased sonication time delivers more energy therefore, creating smaller size of nanoparticle.

3D plot showing the effect between PC-SC, PC-ST and SC-ST have been given away in figure.1.21, 1.22 and 1.23 respectively, where ST is the sonication time, SC is concentration of surfactant and PC is concentration of polymer

Design-Expert® Software

Factor Coding: Actual
particle size (nm)



X1 = A: polymer concentration
X2 = B: surfactant concentration.

Actual Factor
C: Sonication time = 6

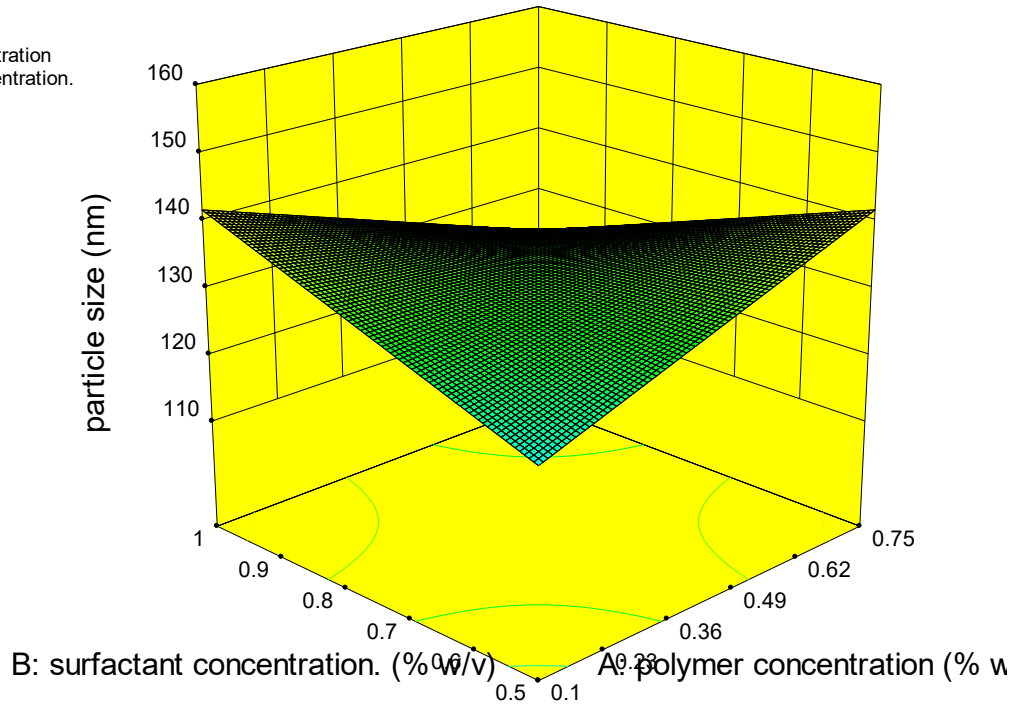


Figure 1.21: 3D response surface plot PC and SC

Design-Expert® Software

Factor Coding: Actual
particle size (nm)



X1 = A: polymer concentration
X2 = C: sonication time

Actual Factor
B: surfactant concentration. = 0.75

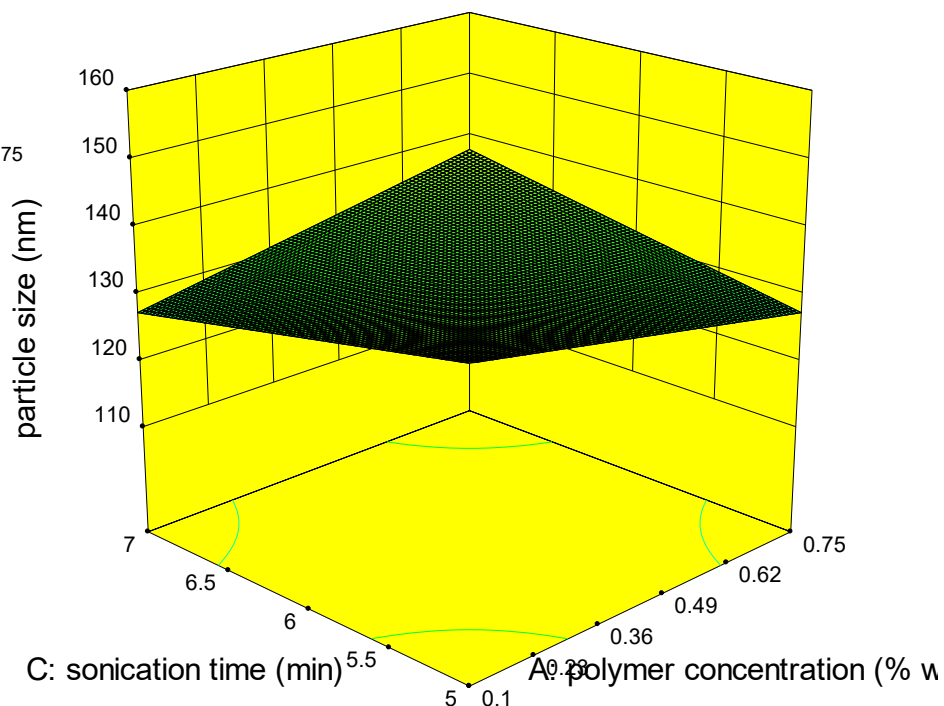


Figure 1.22: 3D response plot between PC and ST

Design-Expert® Software

Factor Coding: Actual
particle size (nm)



X1 = B: surfactant concentration.
X2 = C: sonication time

Actual Factor
A: polymer concentration = 0.425

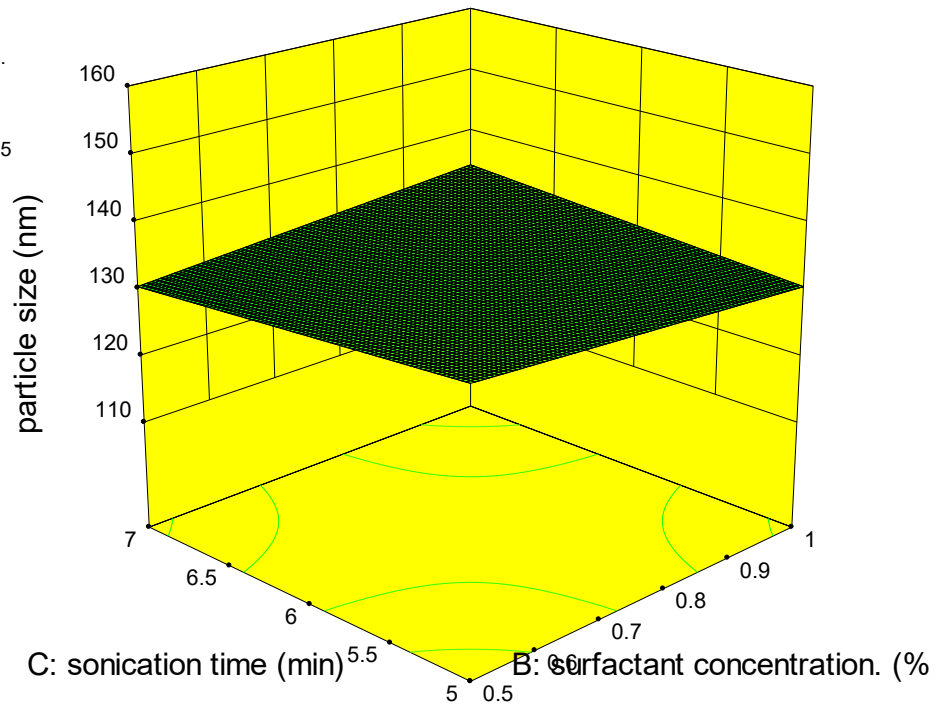


Figure 1.23: 3D surface plot between SC and ST

6.3.2 Result on Entrapment Efficiency:

The entrapment efficiency of 8 batches of BM chitosan nanoparticle ranged from 50.01%±2.1 to 64.11±3.1 % for two level three factor combination. The following quadratic equation described the influence of independent variables on entrapment efficiency.

$$Y_2(\text{EE})\% = 59.57 + 0.11A - 1.99B - 0.35C + 0.98AB - 1.23AC - 1.99BC + 0.70A^2 - 4.38B^2 - 3.40C^2$$

From the equation no.8 it was clear that the coefficient A had a positive effect on Y2 (entrapment efficiency) which clarifies EE% increases with increase in polymer concentration. All the results were significant at $p \leq 0.05$. 3D surface plot on behalf of the influence between PC-SC, PC-ST and SC-ST have been given in figure 6F-17 to 6F-19 for EE% respectively.

Design-Expert® Software
Factor Coding: Actual
Entrapment efficiency (%)



X1 = A: polymer concentration
X2 = B: surfactant concentration.

Actual Factor
C: sonication time = 6

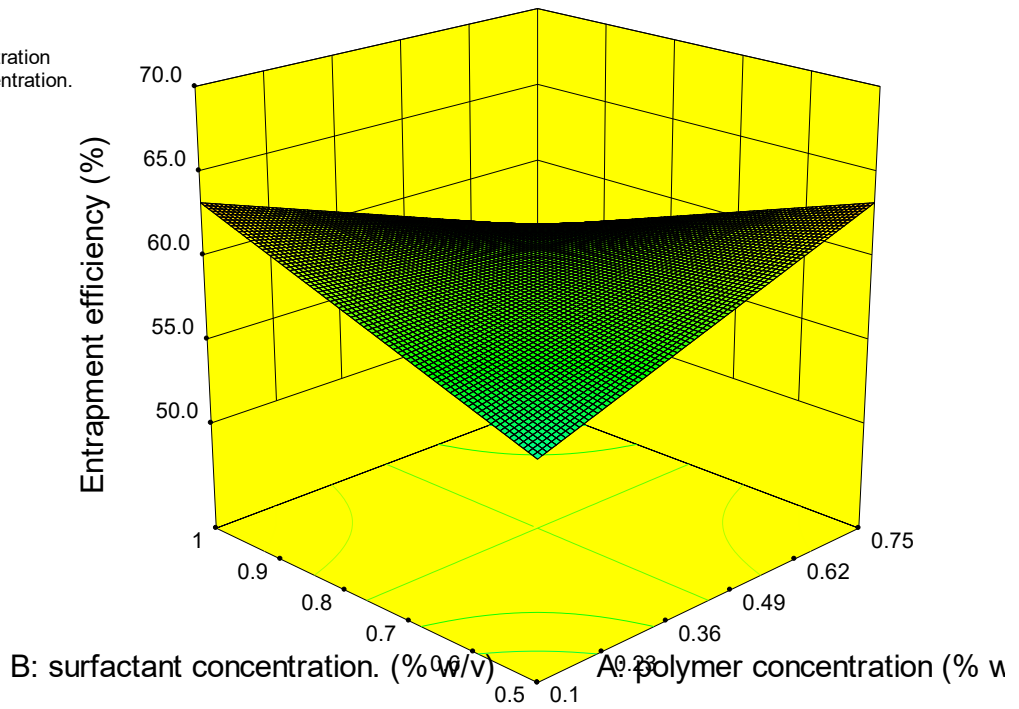


Figure 1.24: 3D surface plot between PC and SC

Design-Expert® Software
Factor Coding: Actual
Entrapment efficiency (%)
66.0
50.1

X1 = A: polymer concentration
X2 = C: sonication time

Actual Factor
B: surfactant concentration. = 0.75

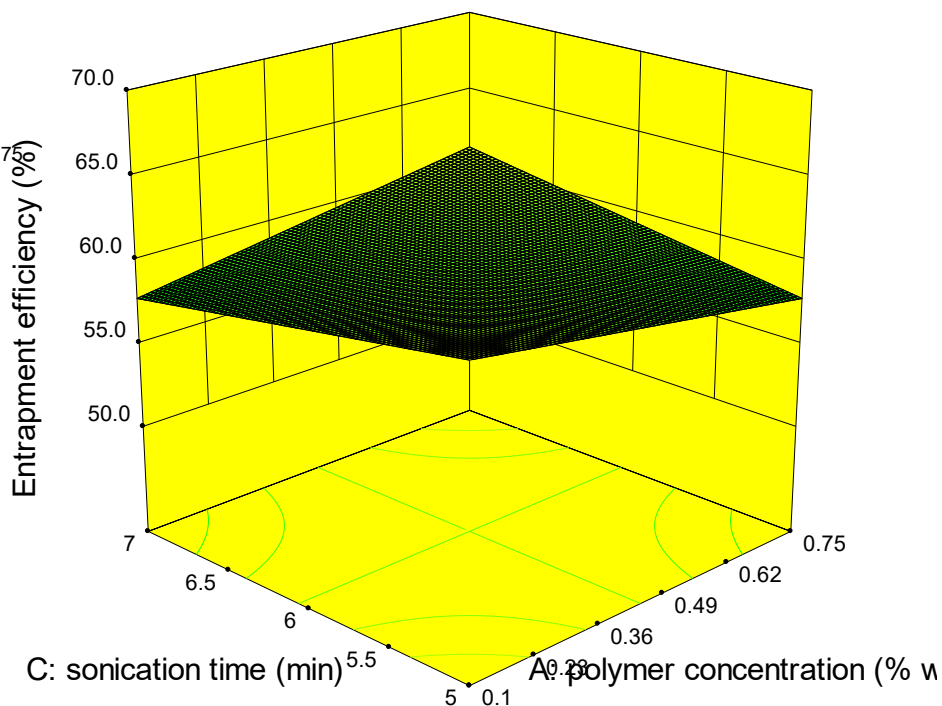


Figure 1.25: 3D surface plot between PC and ST

Design-Expert® Software
 Factor Coding: Actual
 Entrapment efficiency (%)
 66.05
 50.12

X1 = B: surfactant concentration.
 X2 = C: sonication time

Actual Factor
 A: polymer concentration = 0.425

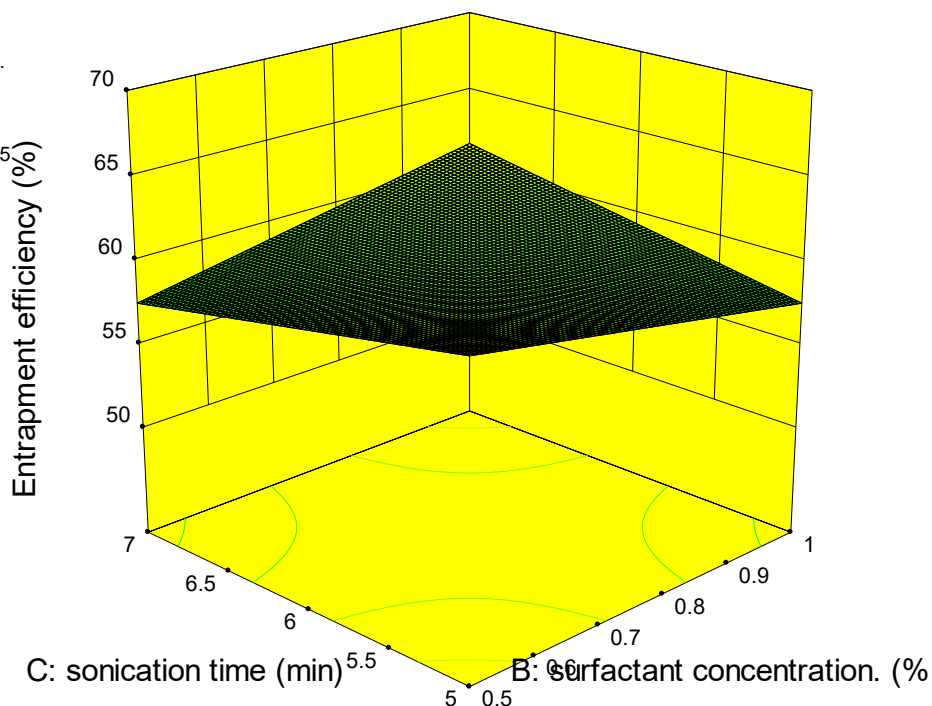


Figure 1.26: 3D surface plot between SC and ST

The design expert version 10 software was used to evaluate the required process for getting best optimized formulation. The optimization results were based on predetermined principle of highest entrapment efficiency and smallest particle size.

It is clear from results obtained in table.1.18 the nanoparticle formulations (NPF-4) prepared with polymer (0.75%) and surfactant (0.5%) concentration respectively, were in desired nano size range (130.27 ± 3.4) and good entrapment efficiency (64.11 ± 3.1) and 6 min sonication time. So, the formulations NPS-4 was considered as optimum formulations and were designated for further studies.

The results of ANOVA model depicted in table 1.20 summary and results of analysis of variance for PS and EE (for BM-CH nanoparticle). The significance of determination coefficient (R^2) and adjusting coefficient were greater than 90% which proves that the model is exceedingly significant.

Table.1.20: Summary and results of analysis of variance for PS and EE (for BM-CH nanoparticle)

Response	Sum of squares	Degree of freedom	Mean square	F value	R^2	Adj. R^2	Perp. R^2
Particle size	1176.23	7	680.62	10.60	0.9972	0.9824	0.9723
Entrapment efficiency	221.52	7	111.23	6.05	0.9921	0.9812	0.9608

6.4 Characterization of Bendamustine loaded chitosan nanoparticle:

6.4.1 Result of Mean Particle Size, Polydispersity Index

The average particle size of blank chitosan nanoparticle 128.24 ± 1.06 and the size of optimized chitosan nanoparticles was $130.27 \text{ nm} \pm 3.4$ with Polydispersity Index (PDI) i.e. 0.245. It is remarkable that particle size of blank nanoparticle is smaller than that of drug loaded nanoparticle. Zeta potential of blank nanoparticle was found around $-19 \pm 0.22 \text{ mV}$ and the drug loaded nanoparticle was around $-21.3 \pm 0.02 \text{ mV}$ with slight increase. The rise in zeta potential may be because of the charge absorbed by Bendamustine particle surface. The negative or positive charge is required for particle repulsion and to make stable nanoparticle as they do not form any aggregates. Figure.1.27 and 1.28 illustrates the narrow particle size range and zeta potential of Chitosan loaded nanoparticle.

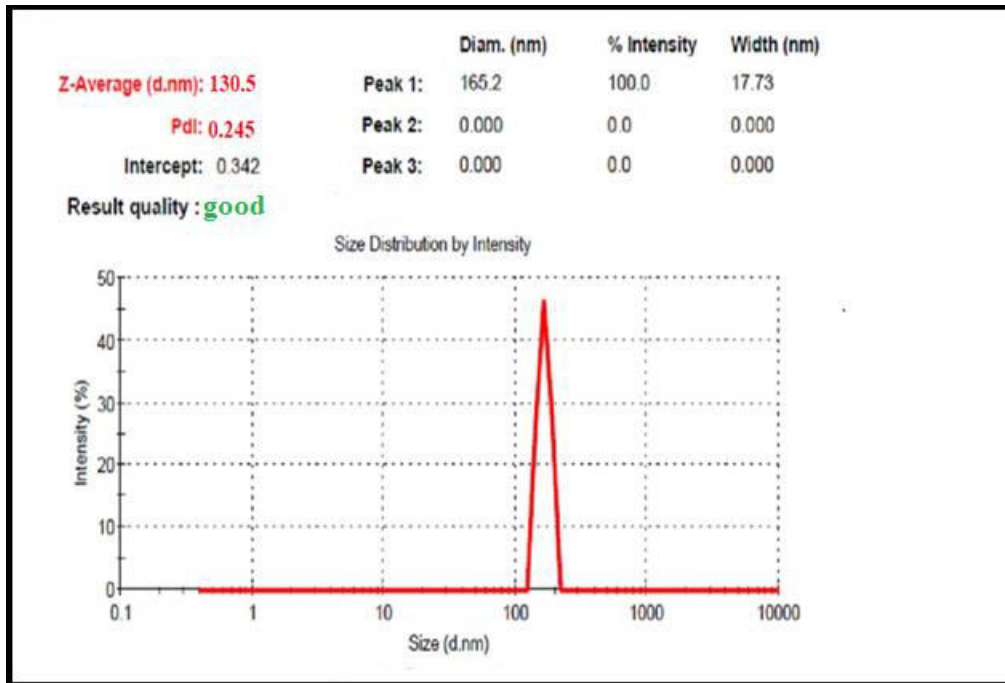


Figure 1.27: Result of Mean Particle Size, Polydispersity Index formulation.no.4

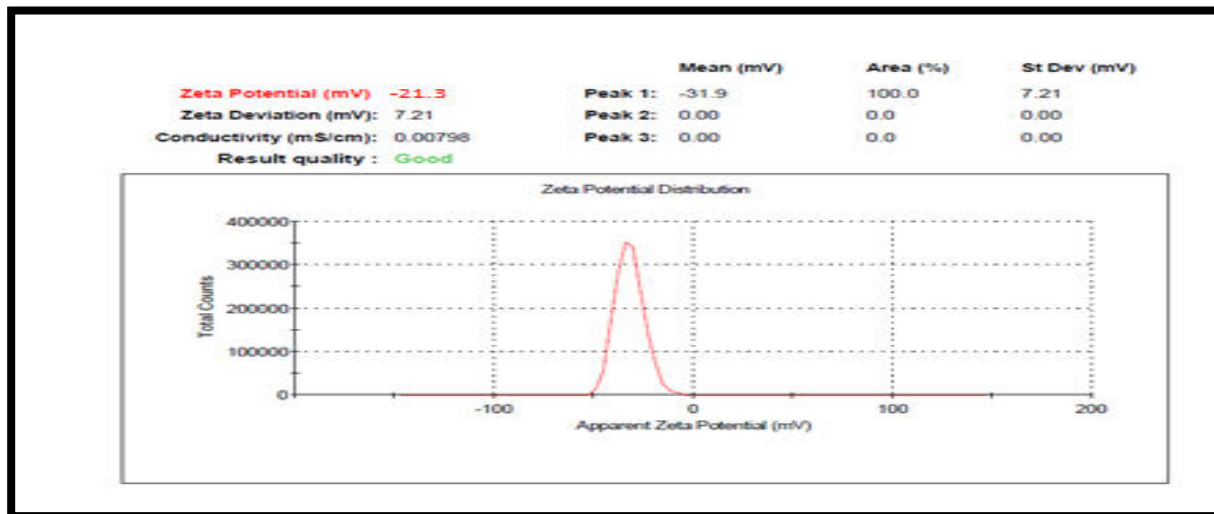


Figure 1.28: Zeta potential of preferred formulation.no.4(Chitosan nanoparticle)

6.4.2 Result of Entrapment Efficiency, Process Yield and Drug Loading Percentage of Optimized Chitosan Nanoparticle

Result of percentage yield of optimized chitosan nanoparticle formulation was $66.20 \pm 0.20\%$, where as the % drug loading of preferred formulation was 25.20% with entrapment efficiency found to be $64.11 \pm 0.13\%$.

6.4.3 Result of Transmission Electron Microscopy of Chitosan Nanoparticle

The TEM was used to determine the particle size, shape, and distribution. Transmission electron microscopy examine images displays the image of nanoparticles that is in spherical shape. Scanned images also confirmed that particles uniform size and polydispersity index with distribution in within the range. All the particles were non-accumulated. The Transmission electron microscopy images are depicted in figure 1.29.

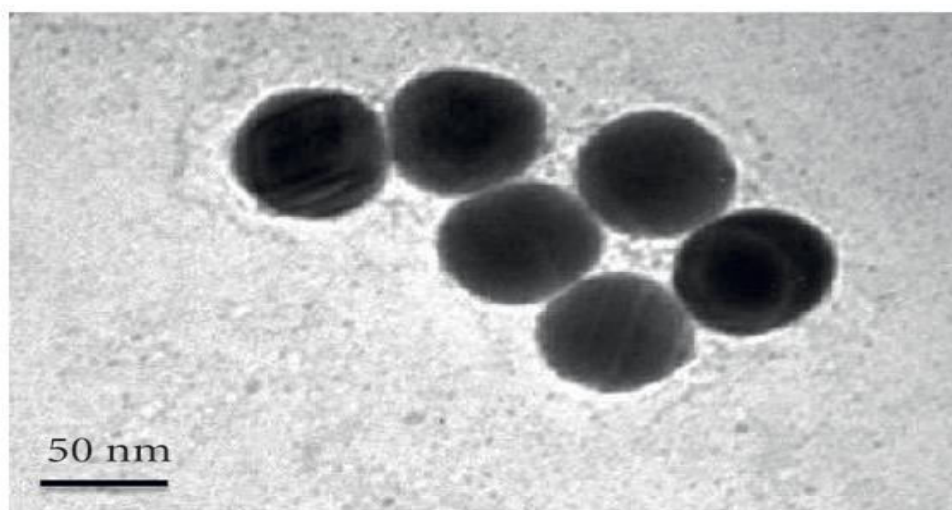


Figure 1.29: TEM image of chitosan nanoparticle

6.4.4 Result of Differential Scanning Calorimetry of Chitosan Nanoparticles

The thermograms of differential scanning calorimetry for chitosan, bendamustine and optimized chitosan nanoparticle (NPS -4) are given in figure 1.30. The active drug bendamustine displayed a narrow peak which resembled its melting point at 155°C , representing that the drug is crystalline in nature. Because of the thermal decomposition of drug, a broad peak was observed with high temperature at around 400°C .

The results of Chitosan polymer showed a broad endothermic peak around 91.26°C . After that exothermic peak started at 270°C . The drug was not showing any endothermic peak in nanoparticle formulation which confirms the amorphous phase and presence of drug in the polymeric nanoparticles.

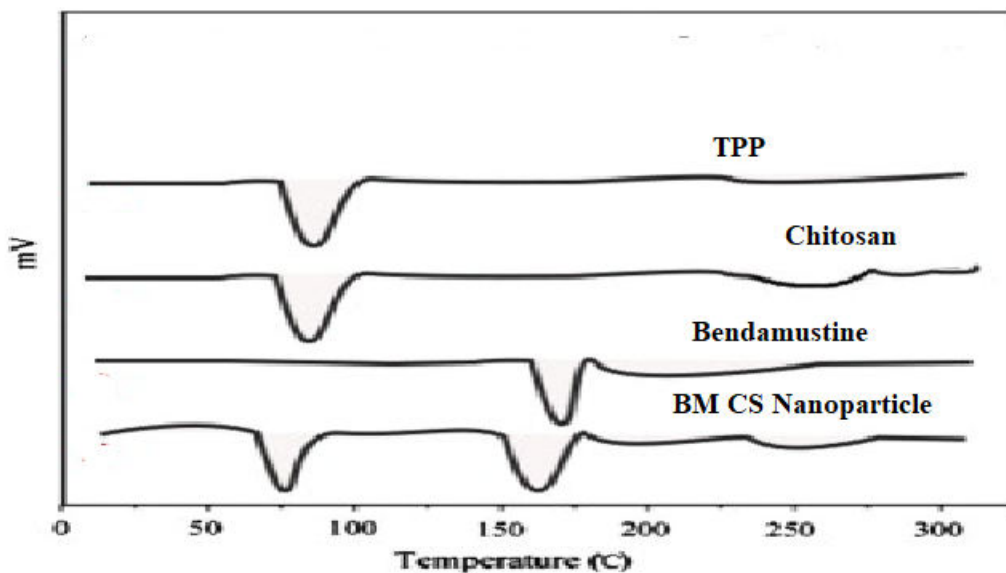
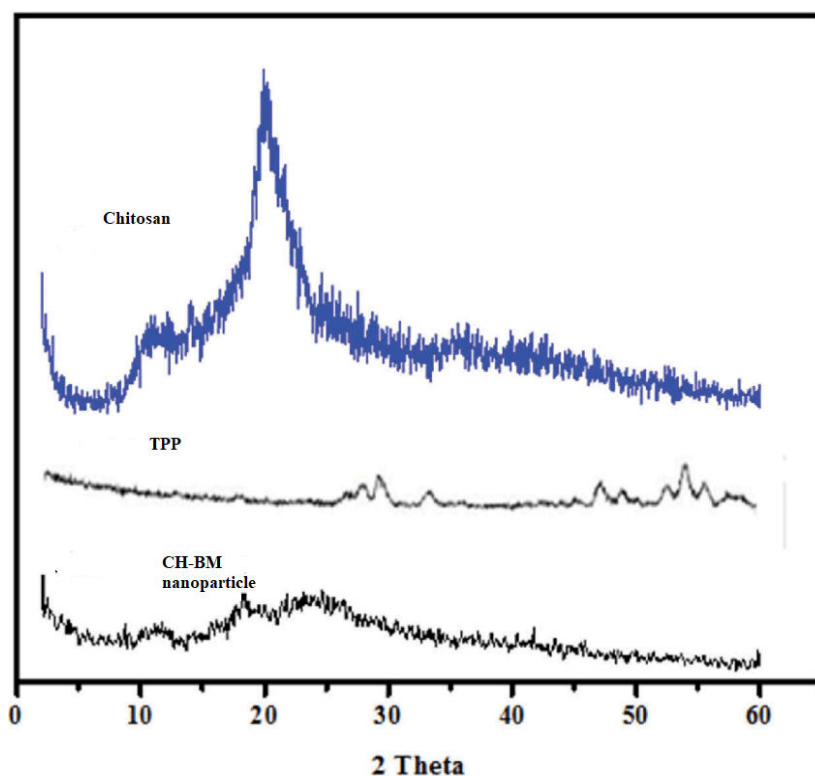


Figure 1.30: DSC Thermogram of TPP, Chitosan, Bendamustine and Chitosan Bendamustine nanoparticle

6.4.5 Result of X-Ray Diffraction Studies

The x-ray diffraction patterns of chitosan, TPP and chitosan nanoparticle were recorded in the fig. 1.32. The pattern of chitosan shows two peaks at $2\theta=10^\circ$ and 20° indicating the crystalline structure of chitosan. Though these peaks become weak as formation of new peaks were observed at $2\theta=11.6, 16.5, 18.2$ and 22.1° . Subsequently, crosslinking with TPP throughout the preparation of chitosan nanoparticles, the crystalline structure of inherent chitosan was demolished and shifting of small peak was observed at $2\theta = 18.85^\circ$.



6.4.6 Result of In-Vitro Drug Release Studies:

The In vitro studies on drug release of bendamustine and chitosan nanoparticles were calculated on the basis of phosphate buffer pH 7.4 and compared through pure suspension of drug for 48 hours and it was observed that BM drug suspension released nearly 99.3% of its pure drug towards the end of 6th hours, though 80.3 % of release was detected at the end of 48th hour from chitosan nanoparticle which displayed steady and sustained release throughout the complete cycle of study. The drug release pattern of chitosan nanoparticle arisen in biphasic way, with an early eruption and rapid release proceeded by sustained release of drug. The result can be seen in table.1.21: results of in vitro drug release of optimized bendamustine and chitosan nanoparticles

Table.1.21: results of In Vitro drug release of optimized bendamustine and chitosan nanoparticles

Time (hrs)	Cumulative percent of drug release of pure BM suspension	Cumulative % drug release (Bendamustine chitosan nanoparticle)
0	0	0
0.5	30.9 ±1.23	20.6± 0.22
1	41.8 ±0.69	47.6± 0.27
2	60.4± 0.11	49.3± 0.18
4	71.1± 0.31	54.6± 0.21
6	99.1± 0.40	58.4± 0.16
8	-	62.6± 0.16
10	-	70.9± 0.20

12	-	72.7± 0.11
18	-	76.9± 0.29
24	-	78.19± 0.24
48	-	80.3± 0.25

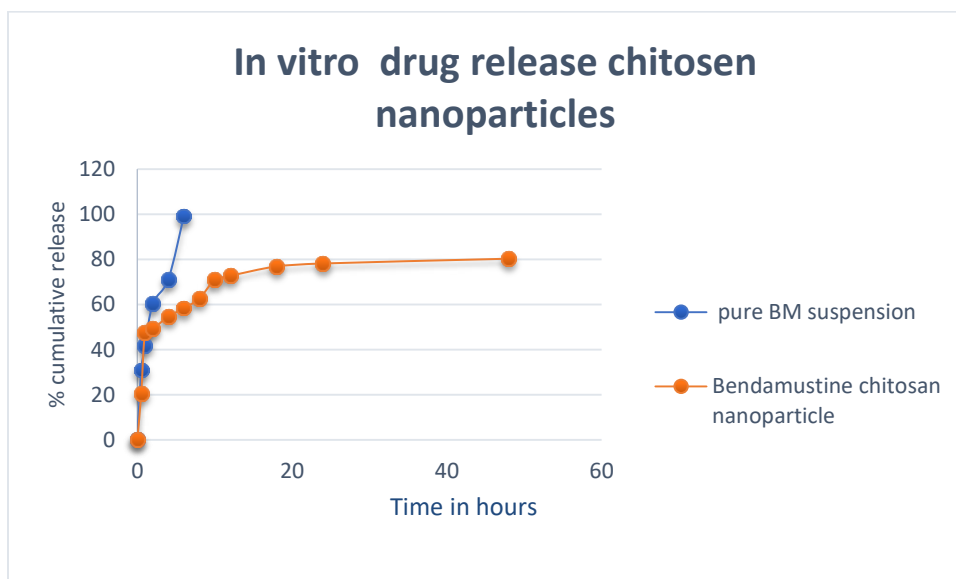


Figure1.32: Drug release study of pure drug suspension and Bendamustine loaded chitosan nanoparticle

6.4.6.1 Result of Drug release kinetics

According to the best fit of ANOVA model and with the uppermost correlation R^2 value (0.96) and the degree of drug release proponent $n=0.78$ that specifies the pattern of drug release is non-fickian and also followed the standard korsmeyer-peppas model. The drug release kinetics result can be seen in table 1.22 drug release behavior of BM from optimized chitosan nanoparticle.

Table.1.22: Drug release behavior of BM from optimized Chitosan nanoparticle

Optimized nanoparticle formulation no.	Zero order		First Order		Higuchi model		Korsmeyer-peppas		
	K	R ²	K	R ²	K	R ²	K	n	R ²
NPF 4	1.3160x10 ⁻¹	0.8195	1.7463x10 ⁻³	0.945	2.178	0.932	5.868x10 ⁻³	0.78	0.96

6.5. Results of Preparation of PLGA Nanoparticles by Solvent Diffusion Technique:

The PLGA nanoparticles were finally prepared by solvent diffusion method were prepared by were successfully prepared by emulsion- solvent diffusion method. The master formula was given in table.1.23.

Table.1.23: The formula for the PLGA Nanoparticles by Solvent Diffusion Technique

	Name of Ingredient	Quantity
1.	Poly(lactic glycolic acid) (Polymer)	3mg/ml
2.	Poly(vinyl alcohol) (Surfactant)	2% w/v
3.	Dichloromethane	10ml
4.	Acetone	10ml
5.	Water	50ml
Conditions		
Stirring speed	500 RPM	
Sonication time	5-7 minutes	
Temperature	Room temperature	

6.6 Optimization of PLGA nanoparticle:

In the Optimization process of PLGA nanoparticle firstly, Preliminary studies were done to determine the suitable range of polymer and surfactant for the formation of nanoparticles (just like chitosan nanoparticle) in the presence of drug. The different concentration of polymer (0.5-3.0 % w/v of PLGA) and surfactant (1.0-2.0 % w/v) were selected for preliminary study for

preparation of PLGA nanoparticles by solvent diffusion technique. Outcomes of preliminary studies within selected range of polymer and surfactant concentration demonstrated two kinds of phenomena i.e., solution, PLGA initial low concentration was 0.5% w/v with surfactants 1% w/v, and the higher concentration of PLGA 3% w/v with surfactant 2 % w/v aggregates or precipitates were obtained.

As founded on the results of preliminary studies, ranges of opalescent parameters were selected as key variables (concentration of Polymer and surfactant) were further examined for formation of optimum PLGA nanoparticle nanoparticles. Table 1.24 The particle size and entrapment efficiency of 8 formulations of nanoparticles were shown in table.1.23 results of PLGA formulated nanoparticles on particle size and entrapment efficiency.

Table1.24: Results of PLGA formulated nanoparticles on Particle size and entrapment efficiency

NSF	Particle size in (nano meter)	Entrapment efficiency in (%)
NPF1	150.9±0.51	81.20±0.04
NPF2	145.2±0.17	80.09±0.07
NPF3	135.6±0.02	79.11±1.03
NPF4	128.2±1.05	76.20±2.31
NPF5	121.3±1.23	74.15±1.12

NPF6	111.2±0.22	70.10±1.03
NPF7	107.6±0.6	60.23± 3.12
NPF8	103.5±0.04	78.13±4.16

6.6.1 Results of BM-PLGA Nanoparticle on Particle Size

The particle size of 8 formulations of BM-PLGA nanoparticle ranged from 103.5±0.04 nm to 150.9±0.51 nm for 3 factor- 2 levels combinations. The influence of independent variables dependent variable i.e. the quadratic equation was designed to describe the particle size.

$$Y_1 \text{ (particle size)} = 115 + 2.165A + 0.740B - 0.672C + 0.94AB - 4.17AC - 6.22BC + 11.30A^2 + 27.06B^2 + 16.12C^2$$

The positive values of factor in the equation show the response factor in the equation specifies that increase in the response variable with the factor. In this A is a polymer concentration which is independent variable had a noteworthy plus positive effect on equation. It also emphasizes that increase in the concentration of polymer raised particle size instantly that is because of during

the emulsification process increase in polymer concentration will increase the viscosity of organic phase which may promote the development of larger size of nanodroplets.

The positive sign of the equation indicates that increased concentration of surfactant may increase the particlesize. Surfactant helps to provide the stability to emulsion nanodroplets and protect them from coalescence with each other. Thus, a smallest quantity of surfactant is essential to get optimum range of nanoparticle².

The 3D response plot was plotted for the effect among ST&SC, PC & S, and SC& PC have depicted in figure 1.33,1.34 and 1.35 respectively; where ST is the sonication time, SC Surfactant concentration and PC is polymer concentration.

Design-Expert® Software
Factor Coding: Actual
particle size (nm)



X1 = A: polymer concentration
X2 = B: surfactant concentration

Actual Factor
C: sonication time = 6

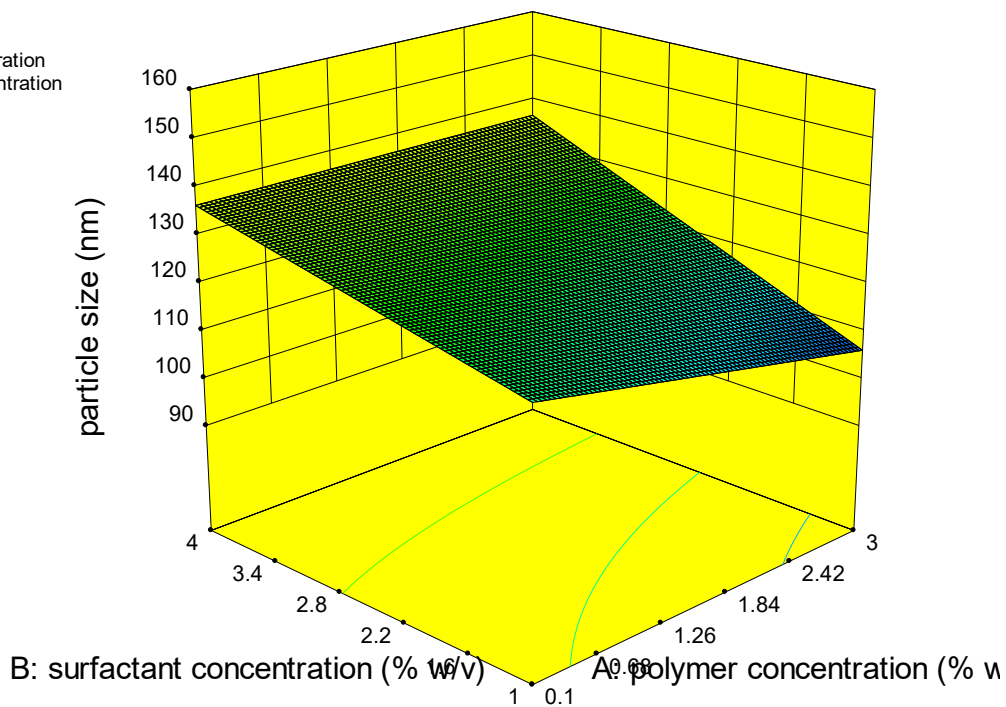


Figure 1.33: 3D surface plot between PC and SC (For BM-PLGA nanoparticle)

Design-Expert® Software

Factor Coding: Actual
particle size (nm)



X1 = A: polymer concentration
X2 = C: sonication time

Actual Factor
B: surfactant concentration = 2.5

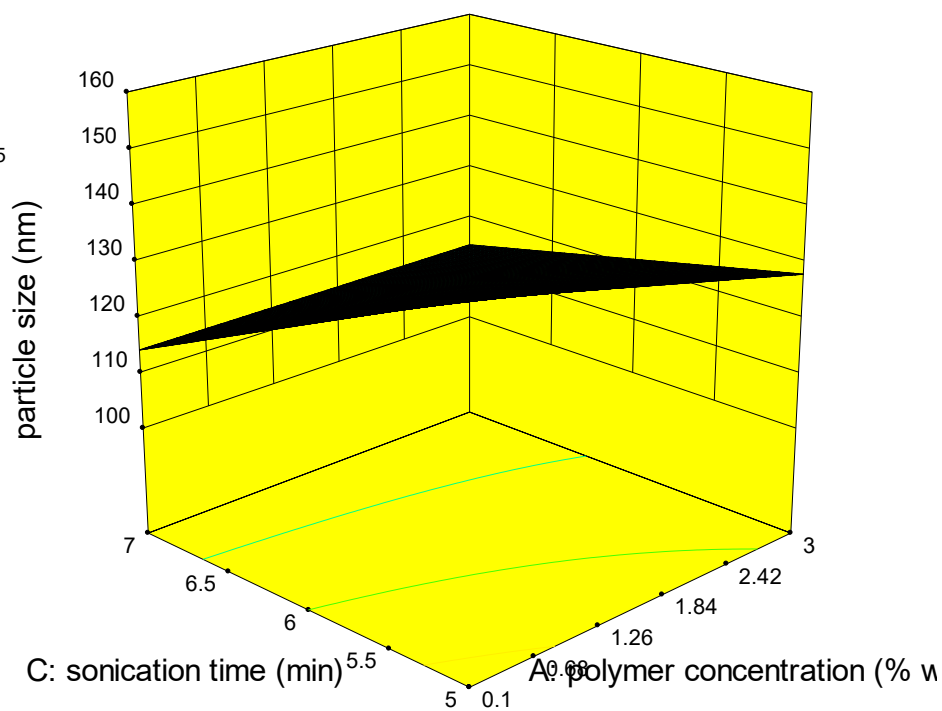


Figure 1.34: 3D surface plot between PC and ST

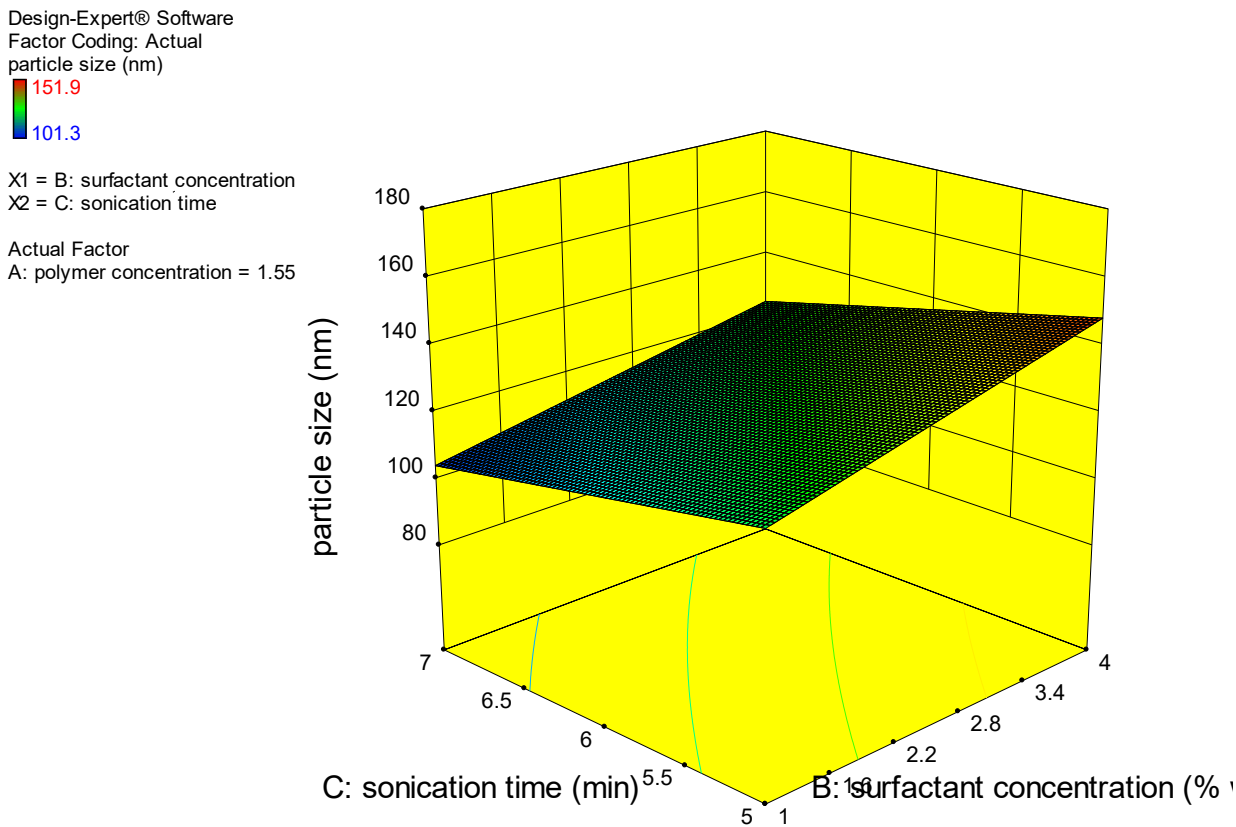


Figure 1.35: 3D surface plot between SC and ST

6.6.2 Results of Entrapment Efficiency of PLGA Nanoparticle

The result on entrapment efficiency of 8 batches was ranged between 58% to 82%. Result was validated through the equation based on independent variable and dependent variables which can be described by following reaction:

$$Y_2 (EE\%) = 75.67 + 3.14A - 1.41B - 1.07C - 0.98AB + 1.26AC - 1.35BC + 0.70A^2 - 4.28B^2 - 3.50C^2$$

Positive sign before A indicates that the entrapment efficiency increases as polymer concentration raised. The negative value before B and C signifies that entrapment efficiency decreases when surfactant concentration and sonication time increases.

All the results were significant at $p \leq 0.05$.

Design-Expert® Software
Factor Coding: Actual
entrapment efficiency (%)



X1 = A: polymer concentration
X2 = B: surfactant concentration

Actual Factor
C: sonication time = 6

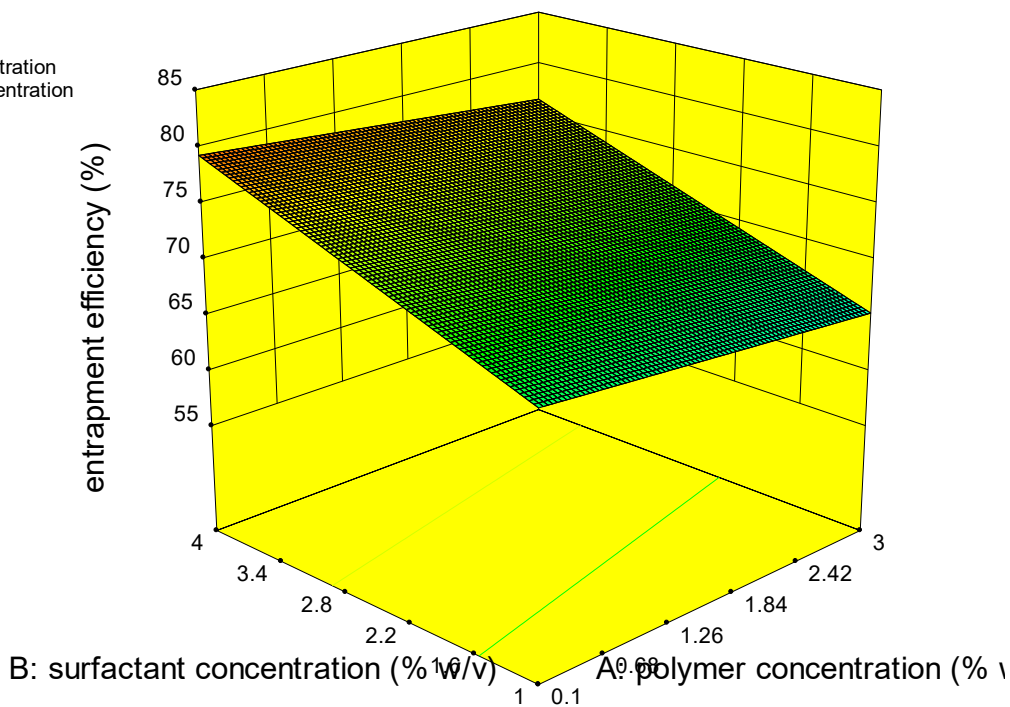


Figure 1.36: 3D surface plot between PC and SC

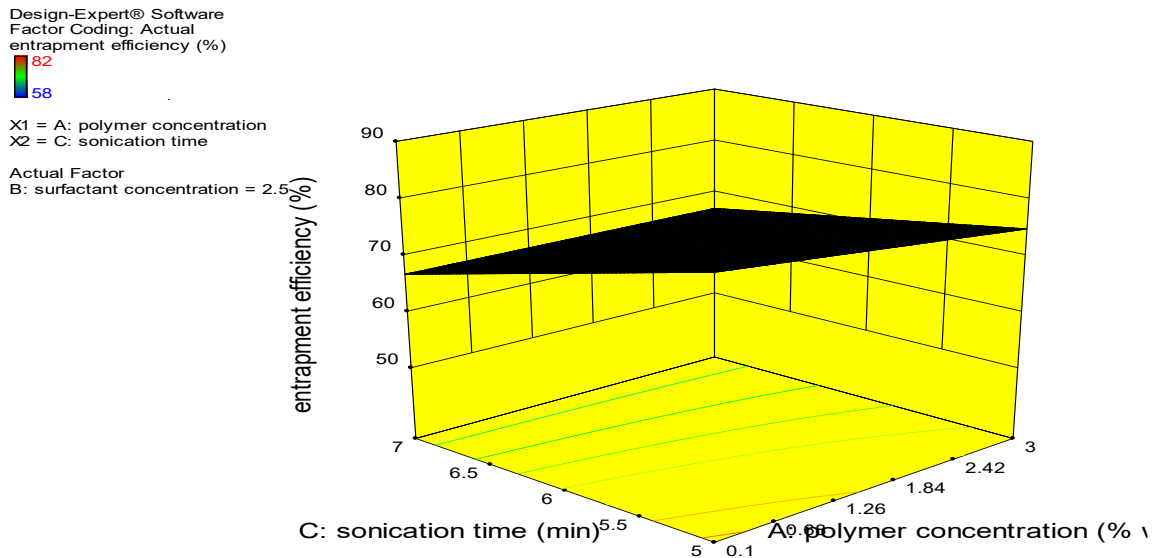


Figure 1.37: 3D surface plot between PC and SC

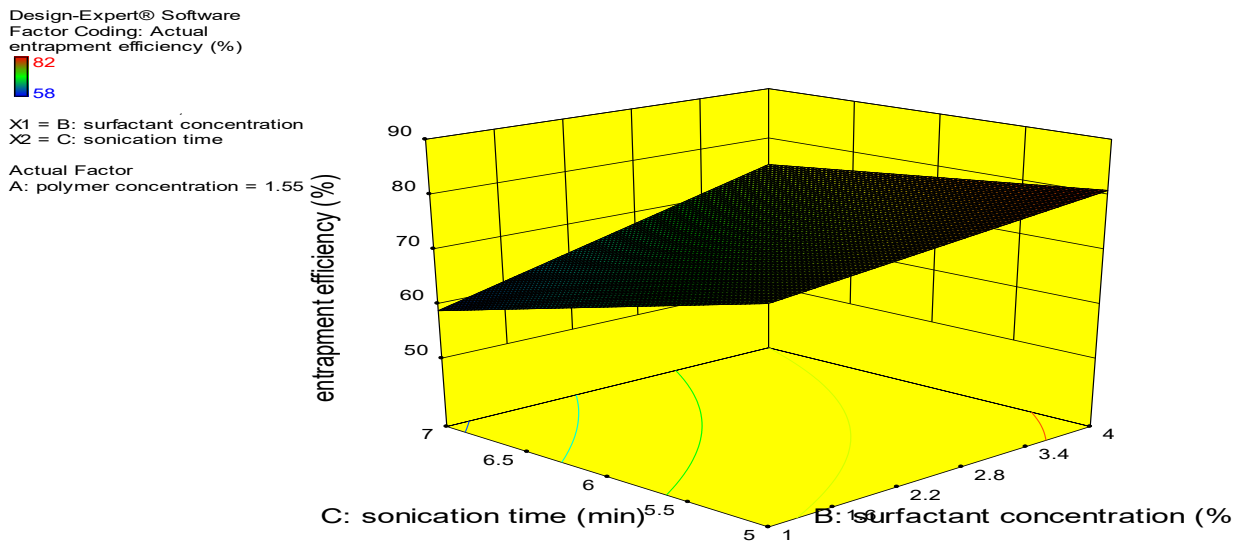


Figure 1.38: 3D surface plot between SC and ST

The particle size and entrapment efficiency for optimized formulations NPF-8 obtained with sonication time 6 minutes were found to be suitable. According to these results, formulation NPF-8 was the optimized formulation with particle size 103.5 nm and 79 % entrapment efficiency. Table 1.25 Summary and results of analysis of variance for PS and EE (for BM-PLGA nanoparticle) based on ANOVA model with significant values. The value of determination coefficient (R^2) and adjusting coefficient were greater than 90% which proves that the model is significant.

Table.1.25: Summary and results of analysis of variance for PS and EE (for BM-PLGA nanoparticle)

Response	Sum of square	Degree of freedom	Mean square	F value	R^2	Adjs. R^2	Perp. R^2
Particle size	2321.46	7	687.38	10.60	0.9948	0.9845	0.9723
Entrapment efficiency	575.88	7	19.01	8.70	0.9807	0.9756	0.9678

6.7 Characterization of PLGA nanoparticles

Results of mean particle size and zeta potential

The particle size of blank PLGA nanoparticle was 101.23 ± 0.04 nm, and the size of preferred formulation loaded with BM was calculated 103.50 ± 0.04 nm with the 0.307 poly dispersity index. It was observed that the particle size of drug loaded PLGA nanoparticles were greater than blank nanoparticles.

The zeta potential for drug loaded optimized nanoparticles was -31.9 ± 3.06 mV. The zeta potential of PLGA nanoparticles were shown in figure 1.39 and 1.40.

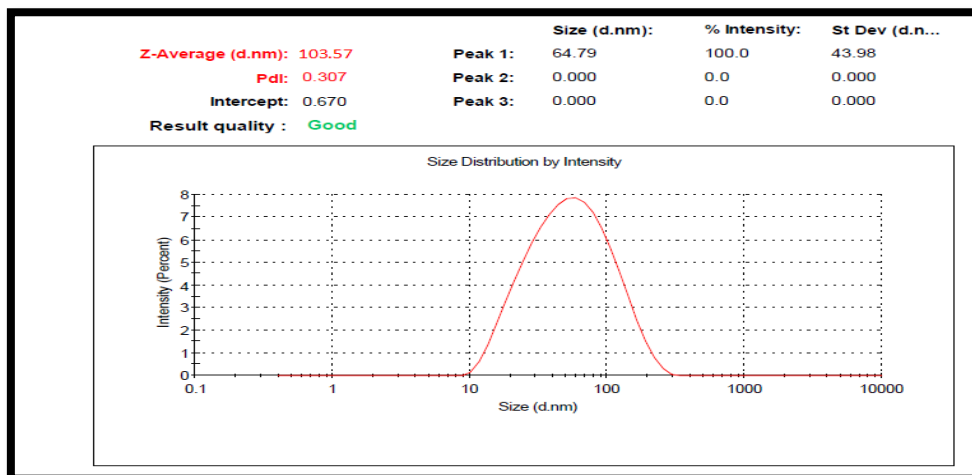


Figure 1.39: Mean particle size of PLGA BM nanoparticle

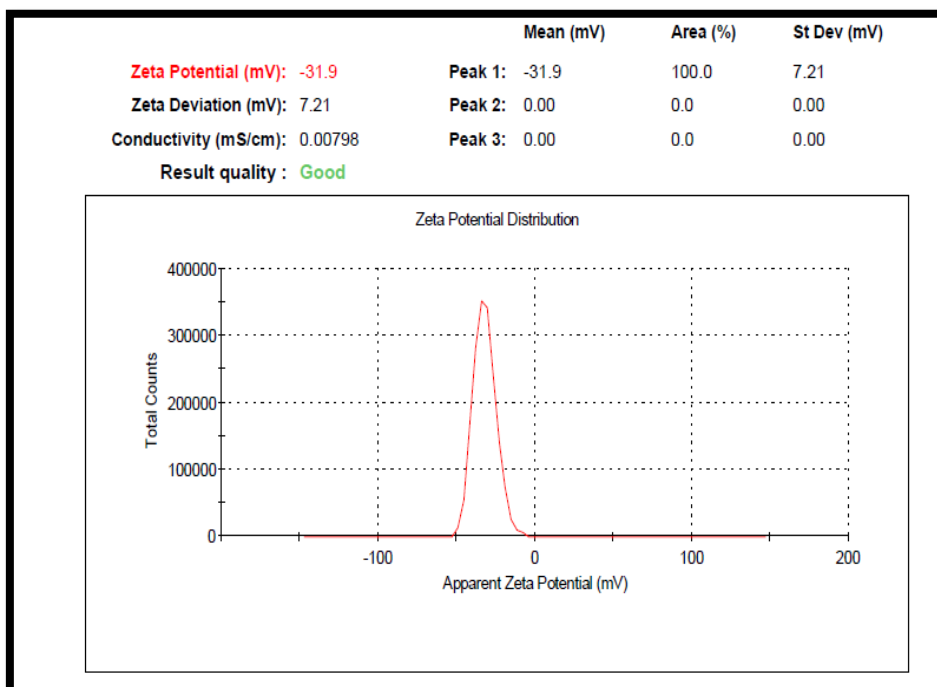


Figure 1.40: Zeta potential of PLGA BM nanoparticles

6.7.1 Results of BM Loaded PLGA Nanoparticle Through Transmission Electron Microscopy

TEM scan displays the development of sphere-shaped nanoparticle. TEM graph also discloses that the particles have a relatively uniform size. The particles were segregated with each other. The dimension of the nanoparticle detected in the graphs were in better arrangement by the information attained from Malvern particle size analyzer. The TEM scan image are characterized in figure 1.41.

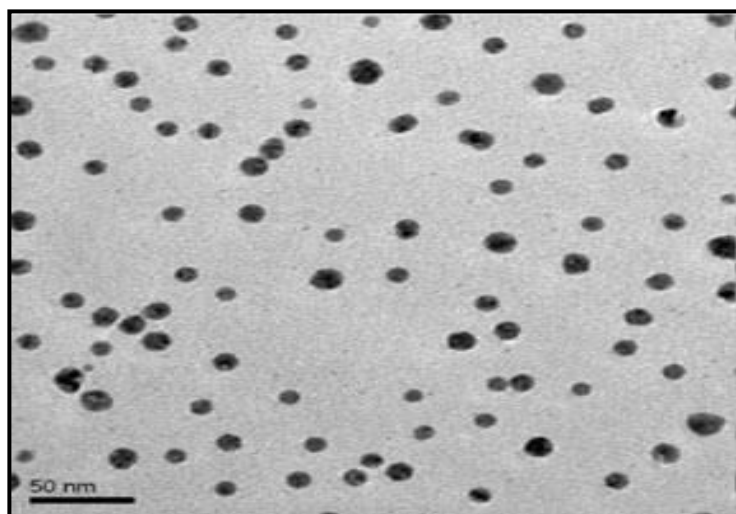


Figure 1.41: TEM image of BM loaded PLGA nanoparticle

6.7.2 Results of Differential Scanning Calorimetry of BM-PLGA Nanoparticle

The differential scanning calorimetry studies of pure Bendamustine, PLGA and bendamustine PLGA nanoparticles shown in fig. no 1.42 DSC thermogram of BM-PLGA nanoparticle. The thermogram of BM were already discussed. The PLGA polymer established a characteristic peak at 45.43°C indicating towards glass transition temperature. The differential scanning calorimetry thermogram of BM-PLGA nanoparticle displayed that polymer is stable up to 250°C with no crystalline material due to nonappearance of sharp peak of bendamustine.

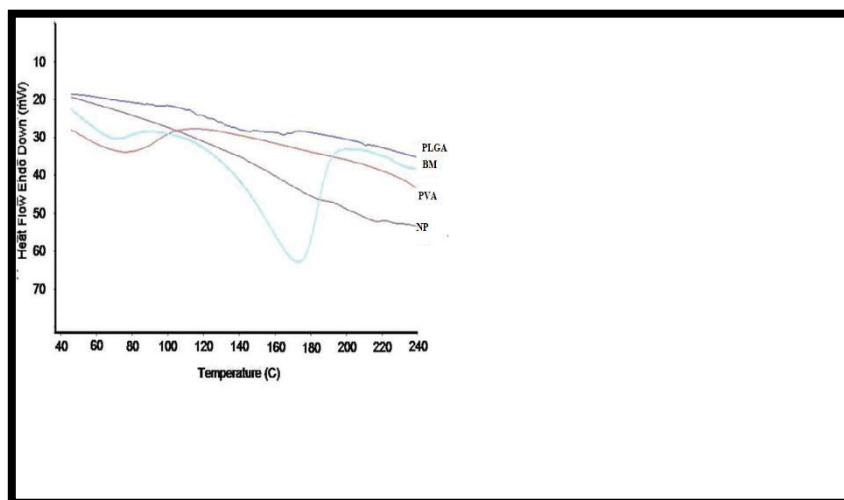


Figure 1.42: DSC thermogram of BM-PLGA nanoparticle

6.7.3 Result of X- ray Diffraction Studies of BM- PLGA Nanoparticle

An x - ray diffraction study of Bendamustine has already studied in prior formulation. In PLGA nanoparticles distorted peak of BM was detected, representing that the pure drug is mixed with

PVA and which does not exist in free form and comparative reduction in the XRD studies. This is due to the variation or decreases in the excellence of crystals of BM and it enhances the change in crystalline form of the drug in amorphous form that helps in solubility enhancement. X-ray diffractogram of pure drug BM, PLGA, PVA and nanoparticle is shown in figure 1.43.

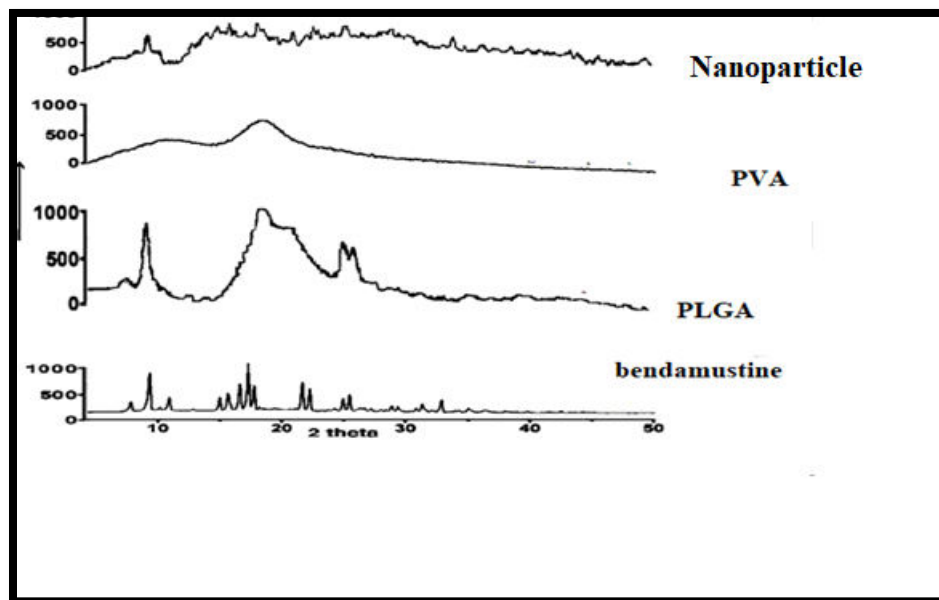


Figure 1.43: X-ray diffraction study of BM- PLGA nanoparticle

6.7.4 Results of In-Vitro drug release of BM Suspension and BM Loaded PLGA Nanoparticles

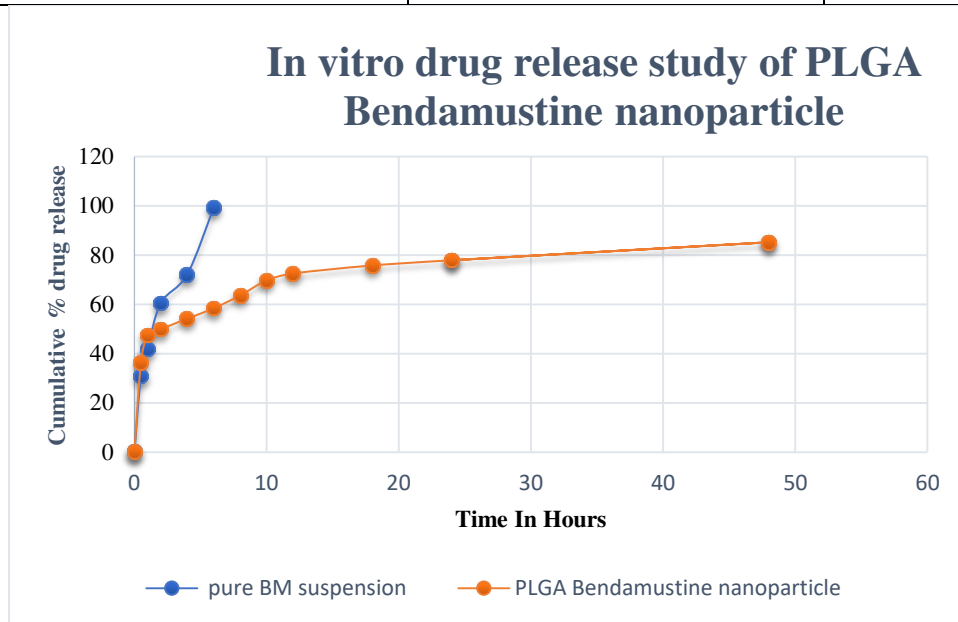
The results of in-vitro drug release of BM suspension and BM loaded PLGA nanoparticles were calculated for 24 hours of duration. The drug release profile was determined in phosphate buffer

At 37°C was given in figure.1.44 and compared with BM pure drug suspension. From the drug release graph, it is sure that pure drug suspension of BM released nearly 98.32% of ± 0.40 of drug towards the end of 6th hours and optimized PLGA nanoparticle released $85.2 \pm 0.24\%$ of drug at its 48th hour. The formulation exhibited a two phase i.e., biphasic release manner with early burst release, and then proceeded by sustained drug release. The preliminary quick release was observed because of drug particles adsorbed in peripheral of nanoparticle surface. All drug molecules dissolved rapidly as they arrive the medium.

Table.1.26: Results of In-Vitro drug release of BM Suspension and BM Loaded PLGA Nanoparticles

Time (hrs)	Cumulative percentage drug release of pure BM suspension	Cumulative percent of drug release of PLGA Bendamustine nanoparticles
0	0	0
0.5	30.9 ± 1.26	36.4 ± 1.13
1	41.8 ± 0.71	47.5 ± 0.20
2	60.5 ± 0.13	49.9 ± 0.59
4	72.1 ± 0.31	54.2 ± 0.05
6	98.2 ± 0.40	58.4 ± 0.28
8	-	63.6 ± 0.18
10	-	69.7 ± 0.19
12	-	72.5 ± 0.04

18	-	75.8 ± 1.03
24	-	77.9 ± 0.02
48	-	85.2 ± 0.24



1.44: Drug release of pattern of BM suspension and BM loaded PLGA nanoparticle

6.7.4.1 Drug Release Kinetics

The optimized formulation of BM-PLGA nanoparticle confirms the first order release pattern in phosphate buffer pH 7.2 as coefficient determination ($R^2 \geq 0.9$). According to the best fit through the maximum R^2 value (0.98) the degree of drug release proponent $n=0.67$ that specifies the pattern of drug release is non-fickian and also followed the standard koresmeyer-peppas model. The drug release kinetics result can be seen in table 1.27 drug release behavior of BM from optimized PLGA nanoparticle.

Table.1.27: Drug release performance of BM from preferred PLGA nanoparticle

Optimized nanoparticle formulation no.	Zero order		First Order		Higuchi model		Korsmeyer-peppas		
	K	R ²	K	R ²	K	R ²	K	n	R ²
Lyophilized formulation of BM-CH	0.0120x10 ⁻¹	0.846	1.3209x10 ⁻³	0.9012	1.902	0.960	5.9492x10 ⁻³	0.674	0.978
Pure BM suspension	0.0189x10 ⁻¹	0.826	1.3101x10 ⁻³	0.9010	1.898	0.940	5.9492x10 ⁻³	0.564	0.965

*K is release constant, R² for coefficient of determination, n is for release exponent

6.8 Formulation and evaluation of dosage form:

6.8.1 Formulation of dry lyophilized powder of Bendamustine loaded Chitosan nanoparticle:

The dry lyophilized powder of chitosan nanoparticle was (NPF.no.4) formulated with mannitol which was used as cryoprotectant. The lyophilized powder (approx. 25 mg) was reconstituted with 10 ml water for injection via shaking. This research showed that no aggregate or clumps were formed during reconstitution with WFI (water for injection).

6.8.2 Evaluation of dry lyophilized powder:

6.8.2.1 Drug Content:

The percentage drug content of lyophilized formulation of BM loaded chitosan nanoparticle was determined by UV-spectroscopic method and was found to be 61.12%.

6.8.2.2 Results of Entrapment Efficiency of prepared Lyophilized Formulation of BM

Observed results suggest that percentage entrapment efficiency reconstituted lyophilized formulation of BM was 64.11%.

6.8.2.3 Results of Particle size, zeta potential of prepared Lyophilized Formulation of BM

The reconstituted lyophilized formulation of BM was found 130.25 ± 3.2 nm with PDI 0.307 and zeta potential of reconstituted lyophilized powder of BM was found -21.3 ± 0.02 mV showed excellent stability.

6.8.2.4 Results of In- vitro drug release studies of prepared Lyophilized Formulation of BM

The in- vitro drug release of prepared lyophilized BM loaded chitosan formulation was significant, shown by graph plotted between cumulative drug release v/s time profile. The percentage of drug release from reconstituted lyophilized powder of BM and the suspension of pure drug BM is given in figure 1.45. Data is shown in table. 1.27.

Table.1.28. Results of In- vitro drug release studies of prepared Lyophilized Formulation of BM

Time (hrs)	Cumulative percentage drug release of pure BM suspension	Cumulative percent of drug release of lyophilized formulation
0	0	0
0.5	30.9 ±1.23	20.6± 0.22
1	41.8 ±0.69	47.6± 0.27
2	60.4± 0.11	49.3± 0.18
4	71.1± 0.31	54.6± 0.21
6	99.1± 0.40	58.4± 0.16
8	-	62.6± 0.16
10	-	70.9± 0.20
12	-	72.7± 0.11
18	-	76.9± 0.29
24	-	78.19± 0.24
48	-	80.3± 0.25

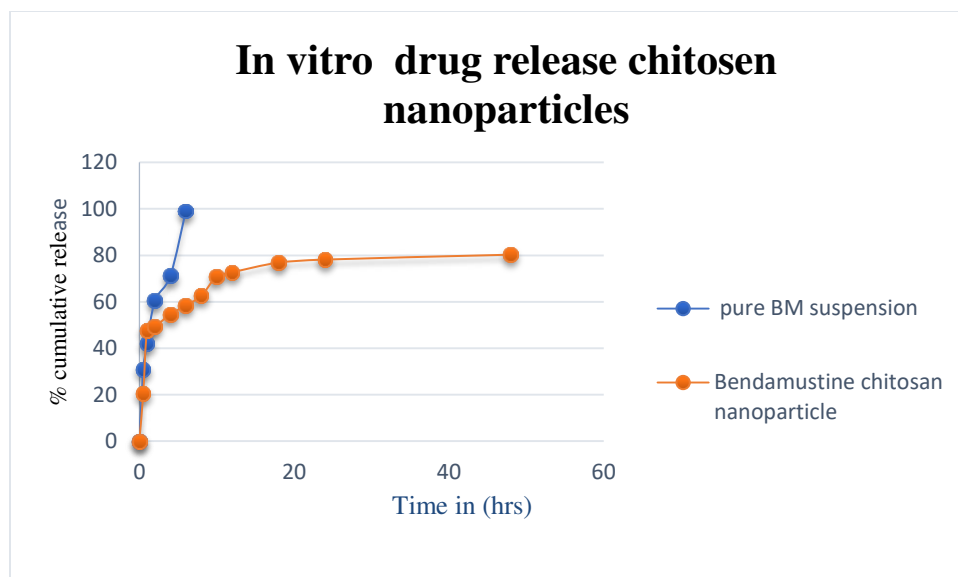


Figure.1.45:Results of In-Vitro drug release of BM Suspension and BM Loaded chitosan Nanoparticles

- **Drug release kinetics of lyophilized formulation of BM-CH**

Based on the results of above graph it has been observed that the lyophilized formulation of BM shown sustained drug release as compared to pure drug suspension. This drug release could be due to the diffusion through polymer matrices. The study specified that pure BM suspension released nearly 99.1% of the pure drug towards the end of 6th hours, whereas 80.3 % release was detected through lyophilized formulation of BM at the end of 48th hours, which displayed the steady release during the whole study. The in vitro drug release profile arisen in biphasic way through a primary eruption (burst) and speedy release stage proceeded by sustained (slower) release stage. The drug release kinetics were studied through estimating the R^2 value. (Shown in table.1.28).

Table.1.29: Drug release behavior of lyophilized BM-CH formulation

Optimized nanoparticle formulation	Zero order		First Order		Higuchi model		Korsmeyer-peppas		
	K	R ²	K	R ²	K	R ²	K	n	R ²
Lyophilized formulation of BM-CH	1.3160x10 ⁻¹	0.8195	1.7463x10 ⁻³	0.945	2.178	0.932	5.868x10 ⁻³	0.78	0.96
Pure drug suspension	1.3060x10 ⁻¹	0.8067	1.7234x10 ⁻³	0.925	2.067	0.912	5.758x10 ⁻³	0.68	0.95

*K is release constant; R² for coefficient of determination, n is for release exponent

The highest value of R² was near about 0.96 for reconstituted lyophilized formulation of BM. That revealed the drug release as of the selected optimized formulation followed the Korsmeyer-Peppas pattern (Table 1.28).

6.8.2.5 Results of In- vitro cellular Cytotoxic study of BM Suspension and BM Loaded chitosan Nanoparticles

The cytotoxic property of pure drug BM loaded chitosan as lyophilized formulation was evaluated by Z-138 cell line. the contact time was 24, 48 and 72 hours MTT assay was used to evaluate the cell viability. The cell viability (IC₅₀) values of pure drug bendamustine and its

lyophilized formulation (NSF-4) was found to be 36.16 ± 0.05 and $18.14 \pm 0.12 \mu\text{m}$ individually next 72 hours contact. The IC_{50} value explains that lyophilized formulation (BM-CH) possesses noteworthy in-vitro anticancer action (antileukemic activity) in comparison with pure drug. No cytotoxic effect was noted when the formulations were exposed to Z-138 cell-line, approved that the formulation is safe.

Table.1.30: The half maximal Inhibitory concentration (IC_{50}) of pure BM suspension also lyophilized formulation of BM-CH on Z-138 cells after 24, 48 and 72 hours.

Cell line	Treatment	$\text{IC}_{50} \mu\text{m}$		
		24 hours	48 hours	72 hours
Z-138	Pure BM suspension	50.6 ± 0.09	48.2 ± 0.12	36.16 ± 0.05
	Lyophilized formulation of BM-CH	46.6 ± 0.21	29.06 ± 1.19	18.13 ± 0.12

The straight contact with drug and cell can cause toxic effects to cell and this might be decreased through incorporation of active drug into the polymeric nanoparticles. All the results reveal that loading of drug into lyophilized formulation powerfully decreased the cellular cytotoxic influence when compared to active drug. The percentage of cell viability at different concentration after 24, 48, and 72 hours are shown from figure.1.46 to 1.48.

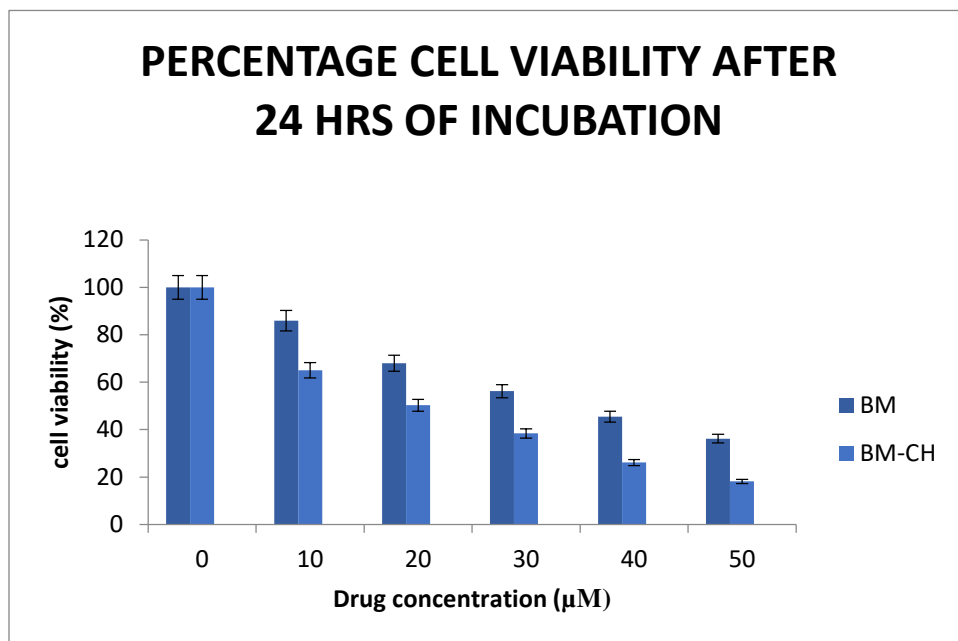


Figure 1.46: Z -138 viability after 24 hours of incubation with pure BM suspension and lyophilized BM loaded chitosan formulation

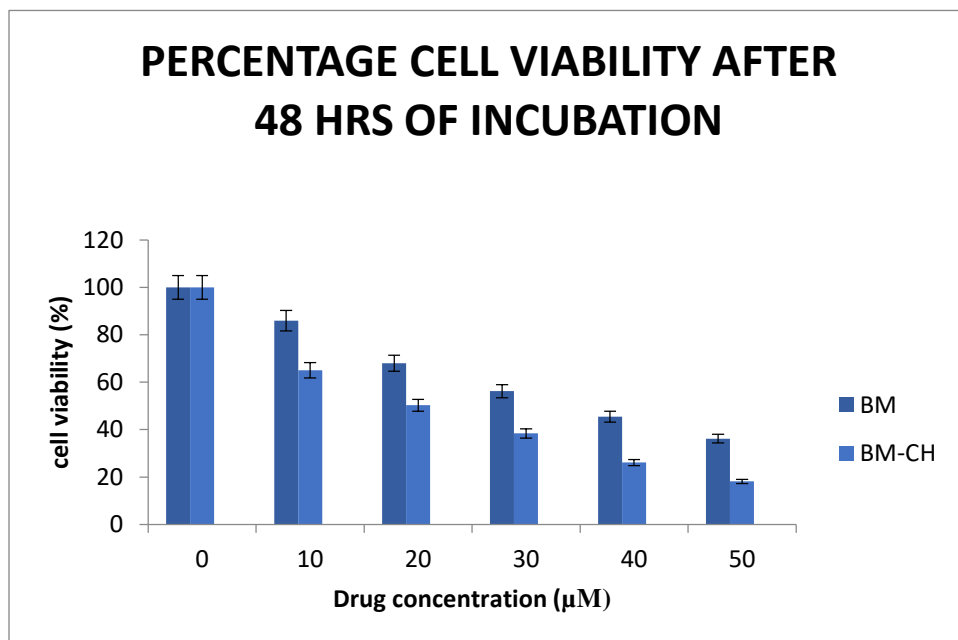


Figure1.47: Z -138 viability after 48 hours of incubation with pure BM suspension and lyophilized BM loaded chitosan formulation

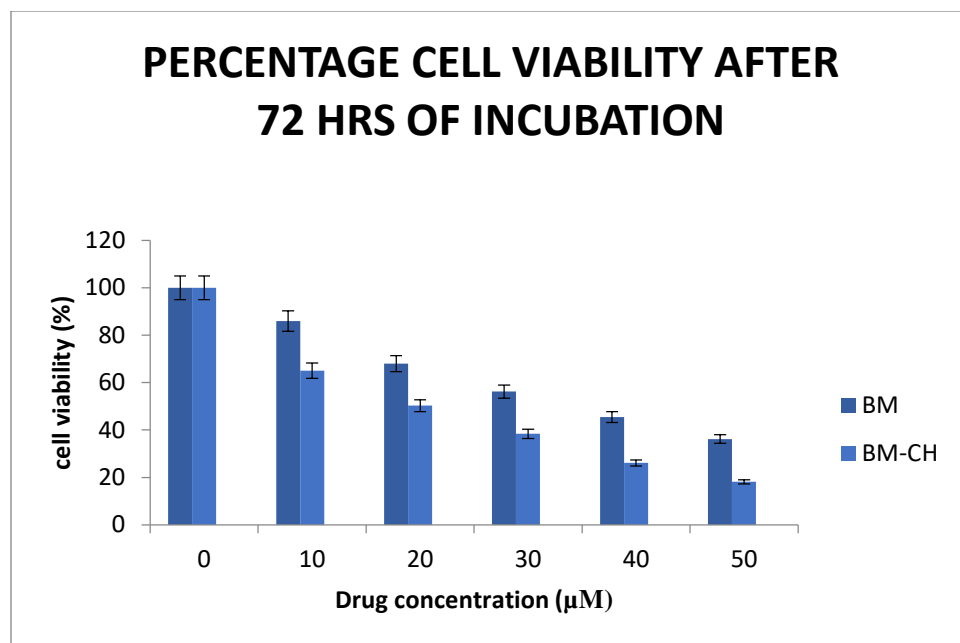


Figure 1.48: Z -138 viability after 72 hours of incubation with pure BM suspension and lyophilized BM loaded chitosan formulation

6.8.3 Stability study:

In stability testing it was observed that the lyophilized powder of BM, degraded about 0.06% of its amount in initial month and 1.03% during 6th month once kept on room temperature ($25^{\circ}\pm 2^{\circ}\text{C}$, $60\pm 5\% \text{RH}$). In the accelerated stability condition ($40^{\circ}\pm 2^{\circ}\text{C}$, $75\pm 5\% \text{RH}$) the lyophilized formulation degraded drug above 1.5% in 1st month and near about 2.11% during 6th months (shown in table 1.30).

Therefore, the lyophilized formulation (lyophilized powder) of BM was considered to be more stable at room temperature when compared to the pure drug suspension and not any noteworthy deviations were observed in particle size, Zeta potential and drug content. The

effect of storage conditions in % residual drug content of BM lyophilized formulations is given in figure 1.49.

Table.1.31: Effect of storage condition on % residual drug content of BM

Formulation code	Room temperature			Accelerated condition		
	% Residual drug content					
	1M	3M	6M	1M	3M	6M
Lyophilized formulation of BM-CH	61.06	61.03	60.03	60.56	60.45	58.45
Pure BM suspension	60.12	60.06	59.06	58.62	58.60	56.62

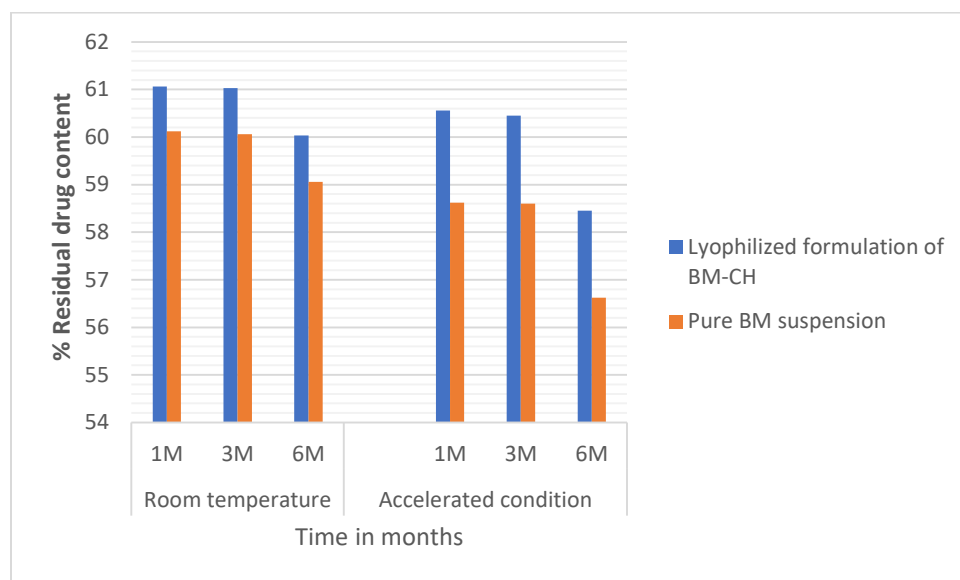


Figure 1.49: Effect of storage conditions on percent residual drug content of pure drug suspension and lyophilized formulation of BM-PLGA

6.9 Formulation of BM loaded PLGA lyophilized powder

The dry lyophilized powder of BM-PLGA nanoparticle was (NPF.no.8) formulated just like chitosan BM loaded lyophilized powder using mannitol as cyroprotectant and WFI

6.9.1 Evaluation of BM-PLGA lyophilized powder:

Percentage drug content: The percentage drug content of lyophilized formulation of BM-PLGA was estimated by UV-spectroscopic method and was found to be 75.28%.

6.9.1.1 Entrapment efficiency:

The percentage entrapment efficiency of reconstituted lyophilized formulation of BM loaded PLGA nanoparticle was found to be 78.16%.

6.9.1.2 Particle size and zeta potential:

The particle size of reconstituted lyophilized formulation of BM was found to be 103.84 ± 0.91 nm with PDI 0.32. Zeta potential was assessed to get evidence about the surface properties of nanoparticles.

6.9.1.3 In vitro drug release:

The in-vitro drug release manner of prepared lyophilized BM-PLGA formulation signified graphically by plotting a graph between percentage cumulative drug release v/s time profile. According to the graph plotted above, it has been observed that the lyophilized formulation of BM- PLGA shown sustained drug release as compared to pure drug suspension also specified that BM suspension released nearly 99.3% of pure drug towards the end of 6 hours whereas 81.59 % drug release was detected through the lyophilized formulation of BM which exhibited sustained release during the entire process of study.

Table 1.32: Cumulative percent of drug release from reconstituted lyophilized powder of BM and the suspension

Time In Hours	Cumulative % drug release of pure BM suspension	Cumulative % drug release (PLGA Bendamustine nanoparticle)
0	0	0
0.5	30.9 ±1.26	36.4 ± 1.13
1	41.8 ±0.71	47.5 ± 0.20
2	60.5 ± 0.13	49.9 ± 0.59
4	72.1± 0.31	54.2 ± 0.05
6	99.2± 0.40	58.4 ± 0.28
8	-	63.6 ± 0.18
10	-	69.7 ± 0.19
12	-	72.5 ± 0.04
18	-	75.8 ± 1.03
24	-	77.9 ± 0.02
48	-	85.2± 0.24

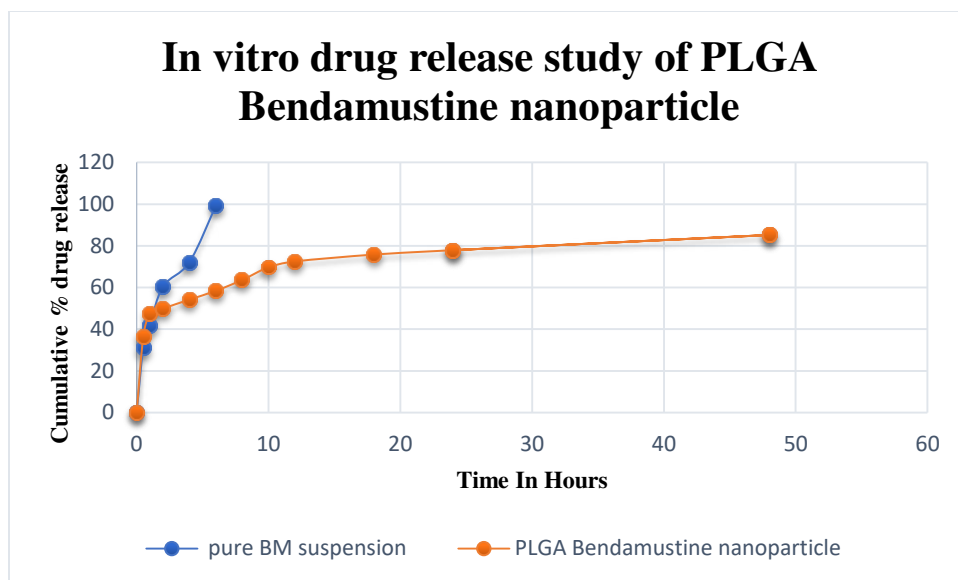


Figure 1.50: Drug release study of pure drug suspension of BM and BM loaded PLGA nanoparticle

6.9.1.4 Drug release kinetics:

According to the bestfit with the maximum correlation coefficient (R^2) value (0.97) and the degree of drug release exponent ($n=0.67$) specifies that the drug release pattern is non-Fickian and followed Korsmeyer-Peppas model. The drug release kinetics of formulation were studied through estimating the R^2 value of different mathematical models. (Shown in table.1.32).

Table1.33: Release kinetics of pure BM suspension and BM-PLGA lyophilized formulation in phosphate buffer.

Optimized formulation no.	Zero order		First Order		Higuchi model		Korsmeyer-peppas		
	K	R ²	K	R ²	K	R ²	K	n	R ²
Lyophilized formulation of BM-CH	0.0120x10 ⁻¹	0.846	1.3209x10 ⁻³	0.9012	1.902	0.960	5.9492x10 ⁻³	0.674	0.978
Pure drug suspension	0.0189x10 ⁻¹	0.826	1.3101x10 ⁻³	0.9010	1.898	0.940	5.9492x10 ⁻³	0.564	0.965

*K is release constant; R² for coefficient of determination, n is for release exponent

6.9.1.5 In-vitro cellular cytotoxic study:

The cytotoxic study of pure BM and BM loaded Poly lactic glycolic acid (PLGA) as lyophilized formulation was evaluated with Z-138 cell line. Subsequent 24,48 and 72 hours of contact. MTT assay performed for cell viability and maximum inhibitory concentration value of formulations were calculated.

The maximum inhibitory concentration values (IC₅₀) of pure drug Bandamustine and its lyophilized formulation (NPF-8) was found to be 36.17 ± 0.05 and 16.13 ± 0.12 μm individually after 72 hours cell contact to drug. The values were given in table.1.33, it explains about the lyophilized formulation (BM-PLGA) possesses noteworthy antileukemic action in comparison to

BM suspension. Not any cellular cytotoxic effect had seen which clear cut approves that the formulation is safe.

Table.1.34: The IC₅₀ value of pure drug suspension also lyophilized formulation of BM-PLGA on Z-138 cells after 24, 48 and 72 hours

Cell line	Treatment	IC50 μm		
		24 hrs	48hrs	72 hrs.
Z-138	Pure BM suspension	50.6 \pm 0.09	48.2 \pm 0.15	36.17 \pm 0.05
	Lyophilized formulation of BM-CH	45.6 \pm 0.21	28.06 \pm 1.19	16.13 \pm 0.12

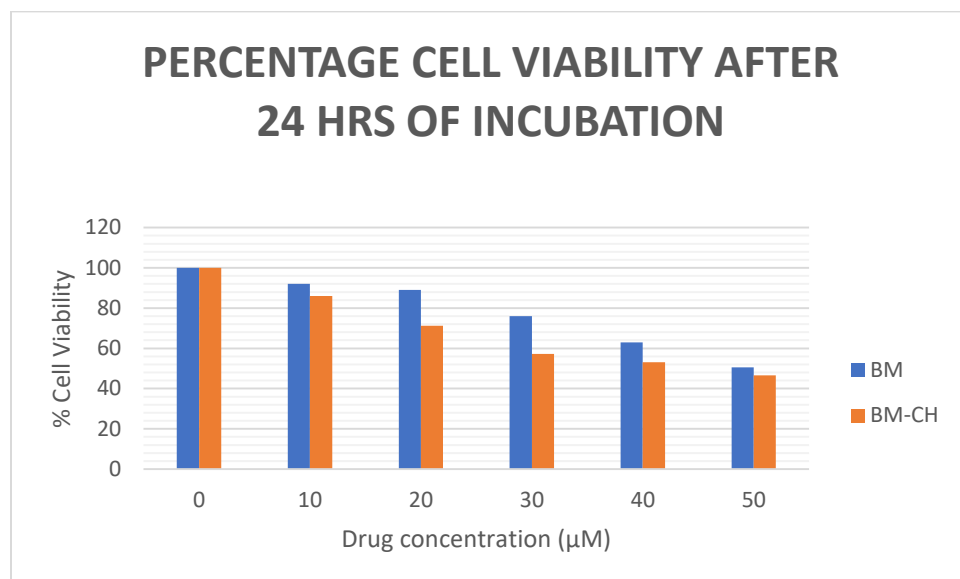


Figure 1.51: Z-138 cells viability after 24 hours incubation with Pure BM suspension and lyophilized formulation of BM-CH

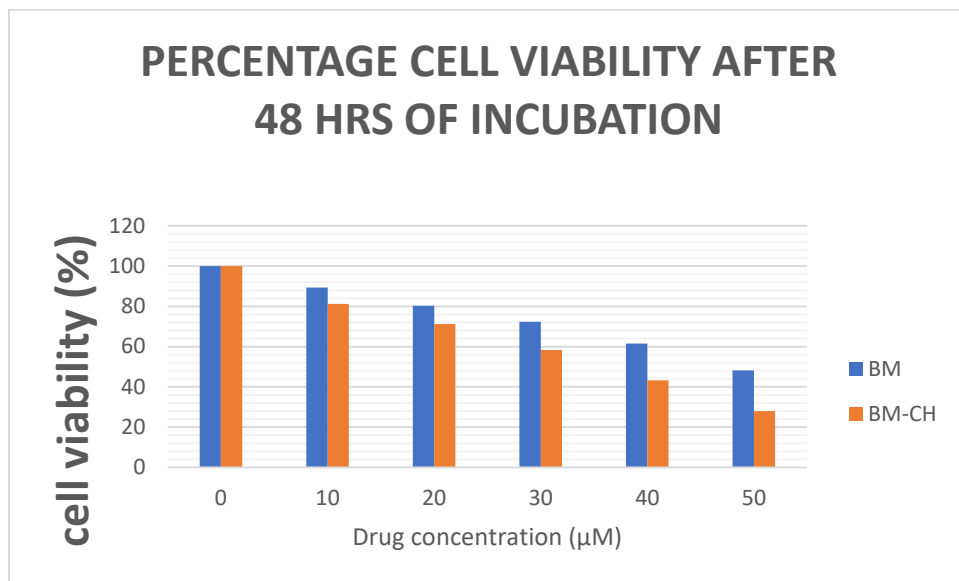


Figure 1.52: Z-138 cells viability after 48 hours incubation with Pure BM suspension and lyophilized formulation of BM-CH

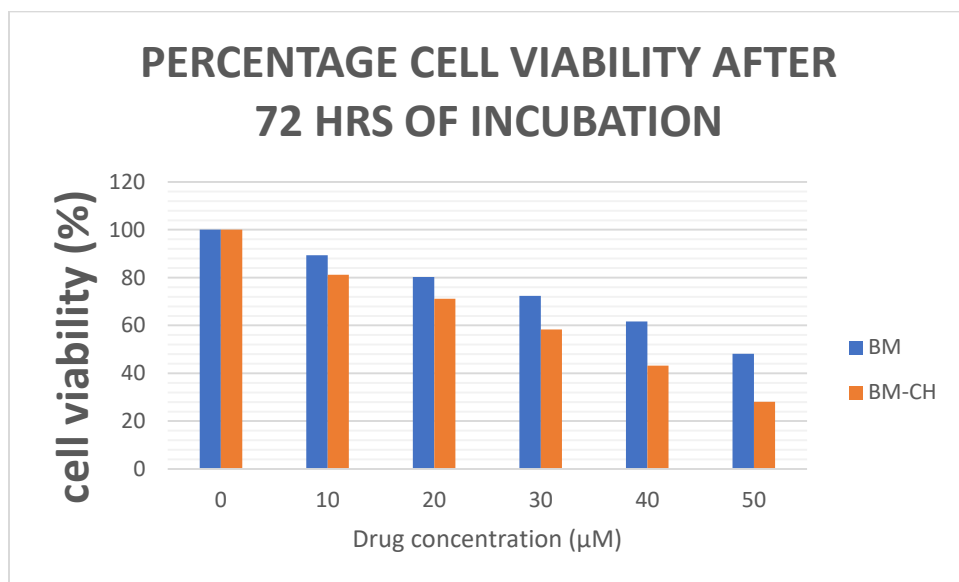


Figure 1.53: Z-138 cells viability after 72 hours incubation with Pure BM suspension and lyophilized formulation of BM-CH

6.9.2 Stability study:

In stability testing it was observed that the lyophilized powder of BM-PLGA degraded nearly 0.03% of active drug amount in initial month and 0.06% in next six months once kept on $25^{\circ}\text{C} \pm 2^{\circ}\text{C}$ room temperature and $60 \pm 5\%$ RH. In the accelerated studies at $40^{\circ}\text{C} \pm 2^{\circ}\text{C}$ and $75 \pm 5\%$ RH the lyophilized formulation degraded around 1.0% drug throughout initial month and near about 1.7% in next 6 months (shown in table.1.34).

Therefore, the lyophilized powder of BM was considered as more stable at room temperature ($25^{\circ}\text{C} \pm 2^{\circ}\text{C}$, $60 \pm 5\%$ RH) as compared to BM suspension and not any noteworthy variations were observed in mean particle size, drug content, and zeta potential. The results were shown in figure 1.54.

Table.1.35: Result of % residual drug content of BM on storage condition

Formulation	Room temperature ($25^{\circ}\text{C} \pm 2^{\circ}\text{C}$, $60 \pm 5\%$ RH)			Accelerated condition ($40^{\circ}\text{C} \pm 2^{\circ}\text{C}$, $75 \pm 5\%$ RH)		
	% Residual drug content					
	1M	3M	6M	1M	3M	6M
Lyophilized formulation of BM-PLGA	75.25	75.20	75.14	74.28	74.25	72.55

Pure BM suspension	60.12	60.06	59.06	58.62	58.60	56.62
--------------------	-------	-------	-------	-------	-------	-------

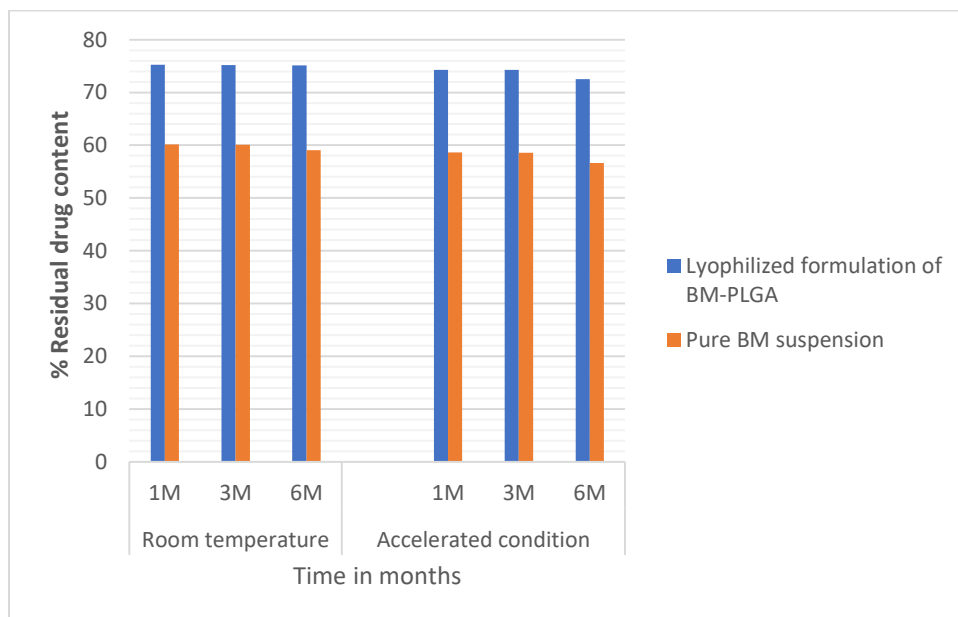


Figure 1.54: Result of % residual drug content of pure drug suspension and lyophilized formulation of BM-PLGA on storage conditions